

Profiling 976 ToxCast Chemicals across 331 Enzymatic and Receptor Signaling Assays

Nisha S. Sipes,* Matthew T. Martin, Parth Kothiya, David M. Reif, Richard S. Judson, Ann M. Richard, Keith A. Houck, David J. Dix, Robert J. Kavlock, and Thomas B. Knudsen*

National Center for Computational Toxicology, Office of Research and Development, U.S. Environmental Protection Agency, Research Triangle Park, North Carolina 27711, United States

S Supporting Information

ABSTRACT: Understanding potential health risks is a significant challenge due to the large numbers of diverse chemicals with poorly characterized exposures and mechanisms of toxicities. The present study analyzes 976 chemicals (including failed pharmaceuticals, alternative plasticizers, food additives, and pesticides) in Phases I and II of the U.S. EPA's ToxCast project across 331 cell-free enzymatic and ligand-binding high-throughput screening (HTS) assays. Half-maximal activity concentrations (AC50) were identified for 729 chemicals in 256 assays (7,135 chemical–assay pairs). Some of the most commonly affected assays were CYPs (CYP2C9 and CYP2C19), transporters (mitochondrial TSPO, norepinephrine, and dopaminergic), and GPCRs (aminergic). Heavy metals, surfactants, and dithiocarbamate fungicides showed promiscuous but distinctly different patterns of activity, whereas many of the pharmaceutical compounds showed promiscuous activity across GPCRs. Literature analysis confirmed >50% of the activities for the most potent chemical–assay pairs (54) but also revealed 10 missed interactions. Twenty-two chemicals with known estrogenic activity were correctly identified for the majority (77%), missing only the weaker interactions. In many cases, novel findings for previously unreported chemical–target combinations clustered with known chemical–target interactions. Results from this large inventory of chemical–biological interactions can inform read-across methods as well as link potential targets to molecular initiating events in adverse outcome pathways for diverse toxicities.



1. INTRODUCTION

Evaluating the safety and hazard of chemicals for potential human health and environmental effects is undergoing a major transformation.¹ This 21st century toxicology paradigm has emerged from the limitations of the current paradigm in regard to cost, time, and throughput, as well as the development of modern biological tools. These tools can probe chemical–biological interactions at fundamental levels, focusing on the molecular and cellular pathways that are targets of chemical disruption.² In this manner, we can begin to understand mechanisms of chemical toxicity that may invoke disease or health effect end points. A more mechanistic understanding will help elucidate common pathways of toxicity and susceptibilities underlying human-relevant outcomes.

Toxicity information is limited or absent for tens of thousands of compounds potentially entering the environment.^{1,3,4} Even for pharmaceuticals designed with a particular biological activity in mind, there is little public information about unexpected toxicities or adverse responses that may be initiated by off-target binding to nuclear receptors, G-protein-coupled receptors, and receptor tyrosine kinases, or by a myriad of events upstream or downstream to receptor engagement.^{5,6}

Evaluating the untested chemicals through the current safety assessment paradigm is limited in throughput, cost, time, and mechanistic revelation. As such, high-throughput screening (HTS) of *in vitro* chemical–target interactions across chemicals, including pharmaceuticals and chemicals of known and unknown toxicities through a broad range of biochemical assays will help describe the chemical–assay space for which there has been no information to date. Our broader hypothesis is that biochemical HTS, when combined with the diverse assays within the ToxCast portfolio, provides an anchor for predictive signatures and mechanistic pathways leading to toxicity. With further analysis, these types of screens may help identify novel initial molecular events potentially associated with pathways of toxicity⁷ and inform systems modeling efforts aimed at characterizing adverse outcome pathways.^{8–16}

EPA's ToxCast project and the federal Tox21 collaboration are generating HTS data and building modeling approaches to identify and characterize biological pathways of toxicity.^{2,3,17} This approach employs a large, structurally diverse chemical

Received: January 14, 2013

Published: April 23, 2013

library to probe a wide spectrum of biological targets and cell-based activities, which enables grouping and prioritizing of chemicals based on their *in vitro* activity profiles, as well as deeper exploration of system biology relationships linking biological activities to *in vivo* toxicology. Further applications of this approach have the potential to enhance and refine structure, metabolism, or presumed mode of action-based read-across methods,¹⁸ as well as to identify potential targets for molecular initiating events in adverse outcome pathways for diverse toxicities. These approaches can be applied to testing prioritization, hazard and safety assessment workflows, design of green alternative chemicals, or screening for adverse effects for drug development processes.

ToxCast Phase I screened 310 unique compounds, mainly food-use pesticides with rich *in vivo* data profiles in 467 biochemical or cell-based assays from 9 assay technologies.^{3,8–16} Despite the somewhat limited chemical diversity of this initial test library, pesticidal compounds were found to have sufficiently rich bioactivity profiles, *in vitro* and *in vivo*, to yield promising new insights and initial predictive models. To expand on these efforts, ToxCast Phase II has significantly broadened the scope and diversity of the chemical library with 667 newly added chemicals, selected based on factors such as production volume, potential for human exposure, possible hazards to human and ecological populations, and availability of *in vivo* toxicity data. Some of these chemicals have known biological activities, whereas most have limited toxicity data as compared to Phase I or have not been previously characterized. Specifically, mammalian biological data, including toxicity, are publically unavailable for the majority of these chemicals. The Phase II chemical set includes phthalates, alternative plasticizers, antimicrobials, pesticides, food additives, toxicity reference compounds, and 111 failed drugs donated by six major pharmaceutical companies.

Previously, we reported an analysis of the original ToxCast 310 Phase I chemical set (PhaseI_v1) in a biochemical screen consisting of 292 protein targets (note: ToxCast Phase I originally reported results for 309 unique chemicals. Upon further review, 2 compounds previously labeled as separately sourced replicates were found to be distinct stereoisomers, yielding a revised total of 310 unique chemicals).⁹ The assays were selected from a commercial NovaScreen panel (NVS) for preclinical drug development. These assays measure chemical binding to nuclear receptors, G-protein-coupled receptors (GPCR), transporters, and ion channels, and enzymatic inhibition or activation for a range of proteins including kinases, phosphatases, CYP450s, proteases, and histone deacetylases. These results are augmented in the present study with newly reported NVS results for the ToxCast Phase II chemical set bringing the chemical inventory to 976 unique chemicals, spanning considerably greater chemical structure diversity and use categories, and with the potential to probe a greater number of biological pathways than Phase I compounds.

This report provides the first critical analysis of findings for 976 chemicals from ToxCast Phase I and II profiled across 331 assays within the NVS panel. The 331 assays evaluated here are currently all of the cell-free assays in ToxCast Phase II. These comprise most of the cell-free assays run in Phase I, with the addition of one new assay (hCAR_Agonist).⁹ The rationale for assay selection was addressed in the Phase I article, and the reduced number of assays in the present study reflect the elimination of assays shown to have lesser value based on

redundancy (i.e., a subset of cytochrome P450s, CYPs) and first-generation predictive models. We focused on relative specificity toward different assay types and their sensitivity to different chemical classes, extending the Phase I study of 310 chemicals. In addition, assays and chemicals were analyzed for similarity based on the chemical–assay activities. Chemical activity similarities were further characterized by enriched chemical structure fragments. Results demonstrate that this large, *in vitro* chemical–target inventory contains potential novel interactions for many unknown chemical–target combinations, as well as off-site targets for some well-characterized compounds.

2. EXPERIMENTAL PROCEDURES

2.1. Chemical Library. Phases I and II of the ToxCast chemical library considered in this study contain 1020 diverse compound samples, consisting of 976 unique structures, and 44 replicate samples for quality control purposes. These chemicals more specifically correspond to the ToxCast PhaseI_v1 and Phase IIa,b chemical libraries. The rationale for chemical selection was based on several criteria, including chemical nominations within the EPA and other federal agencies (e.g., National Toxicology Program/National Institutes for Environmental Health Sciences; National Center for Advancing Translational Sciences/National Institutes of Health; U.S. Food and Drug Administration); international organizations such as the Organisation for Economic Co-operation and Development; and other stakeholder groups. The chemical use groups for the nominated chemicals include (but are not limited to) marketed drugs with known target activities and over 100 failed (terminated) pharmaceuticals donated by several pharmaceutical companies; phthalates and alternative plasticizers; antimicrobials; pesticides; and food additives. Other selection criteria included DMSO solubility and compound commercial availability and affordability. A tabular listing and Structure Data Format (SDF) file of the complete ToxCast chemical library, of which the 976 compound library is a subset, is available for download at http://www.epa.gov/ncct/dsstox/sdf_toxcast.html.

2.2. Chemical Quality Control (QC). Chemical information associated with the ToxCast library (i.e., chemical names, CAS RN, and substance description) was quality reviewed and structure-annotated within the U.S. EPA's DSSTox project (<http://www.epa.gov/ncct/dsstox/>). Chemical samples were commercially procured, diluted in dimethyl sulfoxide (DMSO) to a stock concentration of 20 mM, and plated by Evotec (formerly BioFocus DPI, South San Francisco, CA). Analytical QC for the Phase I chemical inventory consisted of high-throughput liquid and gas chromatography mass spectrometry determination of sample purity, parent mass, and sample stability in DMSO over time (<http://www.epa.gov/ncct/toxcast/chemicals.html>). Similar analytical QC methods are being applied to analyzing the Phase II portion of the current ToxCast library in association with the Tox21 project and will be made publically available upon completion. Additional information about these chemicals can be found by querying the DSSTox GSID, from Supporting Information, Table S2, in the publically available DSSTox Structure Browser (http://epa.gov/dsstox_structurebrowser/), which provides additional structure-based link-outs to information in EPA's ACToR database (<http://actor.epa.gov>) and in PubChem (<http://pubchem.ncbi.nlm.nih.gov/>).

2.3. Assay Description. The NVS assays, developed and run by Caliper, a PerkinElmer company (Hanover, MD), consisted of 331 assays that detect whether a test chemical alters the binding of ligands to receptors (131) or inhibits enzymatic activity (100). The 100 inhibitory enzymatic assays were also assessed for enzymatic activation, resulting in an additional 100 assays. Details on individual assays, catalog numbers, quality assurance methods, and literature references can be obtained at www.caliperls.com/products/contract-research/. Supporting Information, Table S1 contains a list of all assays, their technical specifications, and active links to specific assay protocols. The assay distribution by protein family consists of the binding format: 77

G-protein coupled receptors (GPCR), including 32 aminergic GPCRs; 19 nuclear receptors, 10 from subfamily 1 and 9 from subfamily 3 (steroid); 7 ion channels; 13 ligand-gated ion channels (LGIC), including 9 cys-loop and 4 ionotropic glutamate receptors; 11 transporters; and 3 other binding assays (other); and enzymatic inhibition (and activation) format, 37 kinases; 19 phosphatases; 15 proteases; 3 cholinesterases; 10 CYPs; and 17 other enzymes including histone deacetylases, phosphodiesterases, monoamine oxidases, and cyclooxygenases. Most assays use human (240) or rat (60) targets; the remaining assays use bovine (10), guinea pig (10), sheep (4), mouse (3), rabbit (2), mixed rodent (1 rat/mouse), and boar (1) targets. Assays were assigned to assay categories (Table 1) for further analysis.

Table 1. Biochemical Activity Profiles by Assay Category^a

assay category	assays ^b	actives ^c	actives % ^c	AC50s ^d	
				≤10 μM	≤1 μM
activator: cholinesterase	3	1	0.03	0	0
activator: CYP	10	10	0.10	10	7
activator: kinase	37	32	0.09	16	7
activator: other enzyme	16	2	0.01	1	0
activator: phosphatase	19	27	0.15	9	1
activator: protease	15	5	0.03	2	0
cholinesterase	3	151	5.16	50	15
CYP	10	843	8.64	450	129
GPCR (aminergic)	32	1579	5.06	540	148
GPCR (other)	45	1175	2.68	287	55
ion channel	7	226	3.31	83	17
kinase	37	277	0.77	49	10
LGIC (cys loop)	9	109	1.24	35	8
LGIC (ionotropic glutamate)	4	28	0.72	1	0
nuclear receptor (subfamily 1)	10	282	2.89	90	41
nuclear receptor (subfamily 3)	9	393	4.47	144	52
other	3	111	3.79	36	15
other enzyme	17	484	2.92	105	25
phosphatase	19	262	1.41	69	19
protease	15	351	2.40	81	14
transporter	11	787	7.33	271	61
total	331	7135	53.19	2329	624

^aTwenty-one assay categories are defined in the Experimental Procedures section. ^bNumber of assays in each category. ^cActives based on the number of AC50 values recorded within an assay category; active fraction (active %) indicates the percentage of theoretical maximum. ^dNumber of actives recorded ≤10 μM and ≤1 μM, respectively.

2.4. Screening Strategy. The screening strategy for Phase II follows the same protocol as that used with the Phase I chemicals.⁹ For Phase II, all chemicals were initially screened at a single concentration in duplicate (161,700 chemical–assay pairs in duplicate). A single concentration of 10 μM was used for CYP assays and 25 μM for all other assays. Assay–chemical combinations were defined as active in the primary screening if they met a predefined threshold of the mean assay signal differing by at least 30% from the vehicle (DMSO) control signal or the mean assay signal varying by a minimum of 2.0 median absolute deviations from the median (MAD2). From these criteria, 14,961 active chemical–assay combinations were conducted in concentration–response along with 25 inactive chemical–assay combinations (14,986 total chemical–assay pairs ordered, 9% of original single concentration pairs). Each chemical was run in 8 serial dilutions using half-log spacing descending from a top concentration of 50–0.023 μM (or 20 μM–0.009 μM for CYP assays). Consistent with Phase I, lower chemical concentrations were used for CYP assays due

to increased sensitivity to inhibition, as expected for enzymes active against xenobiotic chemicals.⁹

2.5. AC50 Calculation. The raw data (percent activity versus positive control) were received by the EPA and processed within a common custom workflow for all assays within the ToxCast project.¹⁹ All Phase I and II data were subjected to custom curve-fitting algorithms for processing and computing AC50 values (chemical concentration at which 50% of maximum activity is achieved). These algorithms were developed in the open source R language,^{20,21} similar to the analysis used for the Phase I chemicals.⁹ The code and source data are available from the authors upon request. The R scripts utilized a four parameter Hill function to fit the data and included the following assumptions: all concentration responses were assumed to be monotonic; outliers were discounted when there was a monotonic curve; a variable slope was allowed; and negative inhibition (activation) was allowed for enzymatic assays. The asymptotes of the curve were constrained to be between –10 and 10% activity (lower) and 100 and 110% activity (upper), to allow for consistent extrapolation of the AC50 across assay–chemical combinations. AC50 extrapolations were allowed at concentrations 3-fold lower than the lowest concentration tested and 3-fold higher than the highest concentration tested to capture potential activity outside of the tested concentrations. Additional criteria for generating AC50 values included Hill curves r^2 coefficient of determination values ≥0.6, p value ≤0.01 (from a test of significant difference between the top and bottom of the curve fit), and E_{\max} (maximum activity) ≥ 30% baseline activity. To capture activity when a dose–response curve was nonmonotonic or could not be calculated from these criteria, a special case AC50 was assigned to the first concentration when a chemical inhibited an assay by at least 50% at any two consecutive concentrations. Specifically, there were 189 chemical–assay pair special cases, which can be seen from the curve fits provided in the Supporting Information. When chemical–assay data did not meet these requirements, a dose–response curve was not generated, and the chemical was deemed inactive in the assay. In cases where a chemical was tested in both Phases I and II, data were not combined to calculate AC50s due to potential variation during temporally separate experimentation; thus, the lowest AC50 value was taken. AC50 values were transformed to $-\log(\text{AC50}/1000000)$ to reflect potency. Inactive chemical–assay pairs were set at 1000000 μM (1M) before transformation to ensure a potency of zero.

2.6. Clustering. Transformed data (i.e., $-\log(\text{AC50}/1000000)$) were clustered with Partek Discovery Suite 6.6 software (Partek, Inc., St. Louis, MO). Chemical–assay unsupervised hierarchical clustering was performed using Euclidean distance as the similarity metric and Ward's method for assembling clusters. Assay–assay and chemical–chemical similarity matrices were built using Pearson's correlation as the similarity metric and Ward's method for assembling clusters.

2.7. Enrichment Score. In order to identify the assays affected by chemicals clustered together in the chemical–chemical similarity matrix, we developed an assay category enrichment score (ES) for each chemical. The ES scores were calculated for each chemical over the 21 assay categories, showing which categories the chemical is preferentially affecting. Initial $\text{ES}_{c,ac} = \text{avg}(\text{AC50})_{c,ac} / \text{avg}(\text{AC50})_{c,ac_rest}$ where c is a given chemical [1,967], ac is a given assay category [1,21], and ac_rest is all other assay categories not associated with the given ac . For example, if the ac was GPCR_aminergic, then ac_rest would be all assays except GPCR_aminergic and GPCR_other. Each $\text{ES}_{c,ac}$ within an ac is normalized by the maximum ES, i.e., final $\text{ES}_{c,ac} = \text{initial } \text{ES}_{c,ac} / \text{maximum}(\text{ES})_{C,ac}$ where C is all chemicals.

2.8. Chemical Structure Enrichment. Univariate analyses between chemical–assay categories and chemical structure fragments were used to determine chemical structure fragment assay category associations. Chemical–assay category ES scores were calculated as in 2.7 (above), but using only AC50s ≤10 μM (i.e., calculated AC50s >10 μM were assigned an AC50 of zero) to reduce potential nonspecific interactions. Chemical structure fingerprints were determined for all chemicals. A fingerprint is a bit string indicating whether a chemical structure contains a particular chemical fragment.

The fragment libraries used are the FP3, FP4, and MACCS fingerprint sets available with Open Babel,²² PaDEL,²³ and PubChem (<http://pubchem.ncbi.nlm.nih.gov>) fingerprint sets. All fragments are described as SMARTS strings. Fingerprinting was carried out using Open Babel and comparing the fragment SMARTS strings to the chemical SMILES strings. In total, there were 6655 fragments used, but only 2950 fragments were found in at least one chemical structure, and 1907 fragments were found in 5 or more structures. For each fragment–assay pair, a 2 × 2 table was built (have fragment, yes or no vs active in assay, yes or no), and standard statistical metrics were calculated. All univariate associations were used where there were at least 5 true positives (cases where a chemical had a fragment and was active in an assay), and the positive predictive value (PPV) was greater than 0.5. These associations were plotted in Cytoscape: An Open Source Platform for Complex Network Analysis and Visualization (www.cytoscape.org).²⁴ Chemical structures were visualized through MarvinSketch viewer (ChemAxon Ltd.) using the U.S. EPA ACToR Web site (<http://actor.epa.gov>).

3. RESULTS

3.1. Data Overview. Since data analyzed in the present study are a compilation of two temporally distinct phases of testing, Phase I and Phase II, assay performance was evaluated using chemical replicates between phases and within phases, on AC50s up to the highest dose tested. For the 11 chemicals replicated across Phases I and II, there was a 95% concordance over 3045 chemical–assay pairs (2907 concordant, including 100 positives and 2807 negatives). Nine chemicals replicated within Phase II showed 93% concordance over 2079 chemical–assay pairs (1941 concordant, including 27 positives and 1914 negatives). Discrepancies of AC50 activities above 10 μM accounted for 74% of the discordances. All subsequent results described herein aggregate results for the 44 total replicates of 11 Phase I compounds and thus consider the set of 976 unique chemicals among the 1020 chemical sample inventory.

Results are summarized in Table 1 for 976 unique chemical actives tested against the 331 biochemical assay portfolio. Active chemical–assay pairs refer to a recorded AC50 value listed in Supporting Information, Table S2. Overall, 729 of 976 chemicals (75%) were active in at least one assay, and 256 of 331 assays (77%) had at least one active chemical. This yielded 7,135 active chemical–assay pairs out of a maximum of 323,056 possible. The assay categories most affected include GPCR (aminergic), GPCR (other), and CYP categories, with 1579, 1175, and 843 actives, respectively. Limiting the AC50s to a threshold of 10 μM or 1 μM gave 2329 and 624 chemical–assay actives, respectively. The GPCR (aminergic) category had the greatest number of actives at $\leq 1 \mu\text{M}$ (148). A chemical affected 10 assays on average, ranging from 0 (274 chemicals) to 90 (1 chemical). An assay was affected by 28 chemicals on average, ranging from 0 (75 assays) to 264 (1 assay). There were 75 assays not affected by any chemical tested, of which 70 are activator assays measuring increased assay activity.

Chemicals and assays were assessed for their promiscuity and potency (micromolar AC50 value). The 20 most promiscuous chemicals are listed in Table 2. They represented a broad range of chemical categories, including heavy metal chemicals (phenylmercuric acetate, mercuric chloride, tributyltin methacrylate, and tributyltin chloride), surfactants (sodium dodecylbenzenesulfonate, perfluorooctane sulfonic acid, dodecylbenzene sulfonate triethanolamine (1:1)), dithiocarbamate fungicides (mancozeb, maneb, and metiram zinc), and a variety of pharmaceuticals. The 20 most promiscuous assays are listed in Table 3. They represent a broad range of assay categories,

Table 2. Top 20 Most Promiscuous Chemicals^a

	chemical name	AC50s		
		total	$\leq 10 \mu\text{M}$	$\leq 1 \mu\text{M}$
1	phenylmercuric acetate	90	47	20
2	mancozeb	88	41	13
3	gentian violet	86	51	5
4	sodium dodecylbenzenesulfonate	82	19	0
5	tributyltin methacrylate	79	48	12
6	tributyltin chloride	77	45	9
7	mercuric chloride	73	45	14
8	perfluorooctane sulfonic acid	72	13	2
9	{4-[3-(aminomethyl)phenyl]piperidin-1-yl}{5-[(2-fluorophenyl)ethynyl]furan-2-yl}methanone (pharma)	71	25	4
10	dodecylbenzene sulfonate triethanolamine (1:1)	66	7	1
11	SSR241586 (pharma)	66	30	8
12	emamectin benzoate	65	14	2
13	{4-[5-(aminomethyl)-2-fluorophenyl]piperidin-1-yl}(4-bromo-3-methyl-5-propoxythiophen-2-yl)methanone hydrochloride (pharma)	64	19	2
14	(1R)-1-[(ethoxycarbonyloxy)ethyl 1-[[5-(5-chlorothiophen-2-yl)-1,2-oxazol-3-yl]methyl]-2-[[1-(propan-2-yl)piperidin-4-yl]carbamoyle]-1H-indole-5-carboxylate hydrochloride(pharma)	63	29	2
15	maneb	62	31	16
16	SSR150106 (pharma)	62	41	13
17	didecyl dimethyl ammonium chloride	62	30	2
18	zamifenacin (pharma)	60	27	11
19	SSR125047 (pharma)	59	16	3
20	metiram	56	16	4

^aColumns indicate the top 20 most promiscuous chemicals, the total number of calculated AC50s, and the number of AC50s at $\leq 10 \mu\text{M}$ and $\leq 1 \mu\text{M}$, respectively. The number of AC50s corresponds to the number of assays affected by a given chemical at the AC50 value constraint.

including transporters (translocator protein (PBR/TSPO), dopamine, norepinephrine), CYPs (CYP1A2, CYP2B6, CYP2C19, CYP2C9), GPCR (aminergic, 5HT7 and DRD1), GPCR (other, opiate κ and opiate μ), nuclear receptor (subfamily 3, AR and GR), nuclear receptor (subfamily 1, pregnane X receptor (PXR)), ion channel (NaCh), other enzyme (MAOAC), protease (BACE), and other (SIGMA receptor).

Fifty-four chemicals had AC50s at the lowest concentration tested for one or more assays (LCT $\sim 0.009 \mu\text{M}$ for CYPs and $0.023 \mu\text{M}$ for non-CYPs), indicating high potency for these chemical–assay pairs. For many of these chemicals, high potency was observed for two or more assays of the same or related category (e.g., CP-471358 and CP-544439 inhibition of matrix metalloproteinases MMP2, MMP9, and MMP13; chlorpromazine inhibition of GPCR ligand binding activity for DRD1, DRD2s, 5HT2C, Adra1A, Adr1B, and H1 and inhibition of NET transporter binding activity) (Table 4). More than half of the compounds listed in Table 4 have literature references to substantiate these observed chemical–target interactions. Results from the data overview indicate that both broad and specific biochemical activities are detected across 323,056 possible chemical–assay pairs in ToxCast Phases I and II.

The literature evidence also revealed missed chemical–target interactions for 10 of the 54 chemicals. Missed known chemical–target interactions included (1) chemicals that missed one assay within the same category (haloperidol

Table 3. Top 20 Most Promiscuous Assays^a

assay target	assay category	AC50s		
		total	≤10 μM	≤1 μM
hCYP2C19	CYP	264	144	53
hCYP2C9	CYP	152	81	19
rPBR	transporter	147	62	18
hPXR	nuclear receptor (subfamily 1)	140	73	35
hNET	transporter	136	48	13
hPBR	transporter	117	36	5
hDAT	transporter	117	45	7
hCYP1A2	CYP	108	60	16
gDAT	transporter	98	26	4
h5HT7	GPCR (aminergic)	96	35	13
hGR	nuclear receptor (subfamily 3)	96	35	6
hOpiate_mu	GPCR (other)	92	27	5
hDRD1	GPCR (aminergic)	89	36	9
rNaCh_site2	ion channel	87	37	13
hCYP2B6	CYP	81	43	16
gSIGMA_NonSelective	other	80	31	13
gOpiateK	GPCR (other)	75	18	4
rMAOAC	other enzyme	73	15	6
hAR	nuclear receptor (subfamily 3)	73	33	8
hBACE	protease	73	28	3

^aColumns indicate the topmost promiscuous assay targets (corresponding to one assay), the respective assay category, the total number of calculated AC50s, and the number of AC50s affecting the assay at ≤10 μM and ≤1 μM. The number of AC50s corresponds to the number of chemicals affecting a given assay at the AC50 value constraint.

affected all 5HT receptors, except h5HT2A; zamifenacin affected all muscarinic receptors, except hM1); (2) assays with species orthologues which were not affected (CP-105696 inhibited the guinea pig but missed the human leukotriene assay, hLTB4_BLT1; PHA-00554613 inhibited the rat but missed the human neonicotinoid receptor, hNNR_NBungSens assay; and UK-416244 inhibited the rat but missed the human serotonergic transporter, hSERT); (3) specific chemical inhibitors which missed the nonspecific assays (CP-457920 and 2,6-difluoro-5-[3-(2-hydroxypropan-2-yl)imidazo[1,2-b]-[1,2,4]triazin-7-yl]biphenyl-2-carbonitrile inhibited bGABAR α 5 but not bGABAR_Agonist or rGABAR_NonSelective); (4) chemicals that inhibited one or no assays in a category (elzasonan a 5HT1b antagonist did not inhibit any 5HT assays; emamectin benzoate is known to bind to mammalian GABA receptors, albeit at a lower affinity than in insects, but it only inhibited 1/5 GABA assays; 5,5-diphenylhydantoin is a substrate and inhibitor for many CYPs, although it did not inhibit any CYPs in this screen).

Evaluating this list for false negatives (missing chemical–target interactions) is limited by publically available information. To evaluate false negatives and true positives (where AC50s were calculated for known chemical–target interactions) in a systematic way, we chose well-known chemical–target interactions in a specific set of assays. The EPA's Endocrine Disruptor Screening Program (EDSP) has an estrogen receptor reference chemical list of known estrogenic compounds of varying potency and nonestrogenic compounds with categories of potency defined as follows: strong actives

exhibit an effective concentration at 50% maximal activity (EC50) of 10^{-11} M; moderate 10^{-9} to 10^{-8} M; weak 10^{-7} to 10^{-6} M, and very weak >10^{-5} M (<http://www.regulations.gov/#!documentDetail;D=EPA-HQ-OPP-2012-0818-0017>). Twenty-two chemicals in common were evaluated in the bER, hER, and mER assays. We found that all inactives (6), strong actives (3), and antagonists (1) were correctly identified. None of the very weak (3) chemicals were correctly identified, but a majority of the weak positives (7 of 9) were in at least two of the assays. Together, these findings indicate that these data are robust with respect to correctly identifying activity within an assay category for weak to strong inhibitors (77%, 17 of 22) correct using two assays); however, limitations are also realized with respect to potentially identifying very weak inhibitors.

3.2. Hierarchical Clustering. To determine how the chemical–assay space was structured, we performed hierarchical clustering based on chemical–assay potency (Figure 1). Clustering by potency ordered the chemical–assay space into sectors ranging from no activity to high activity. For some clusters, it was possible to annotate by assay category or chemical class (Figure 1A). Figure 1B shows the clustering for 10 of the most promiscuous chemicals including heavy metal chemicals, surfactants, and dithiocarbamate fungicides. Distinct effects can be seen among these chemical classes, indicating some degree of specificity. Four functional categories listed across the top of the hierarchical cluster (pesticides, pharmaceuticals, consumer use chemicals, and phthalates and alternative plasticizers) give a diverse representation of the chemicals evaluated in this data set (Figure 1A). These data show varying degrees of sensitivity and specificity as will be discussed in section 3.3.

Prominent assay clusters containing relatively homogeneous assay categories included GPCR (other), nuclear receptor (subfamily 3), kinase and phosphatase, and GPCR (aminergic) (Figure 1A). The clustering was clearly following at least some of the biology of the constituent chemical–assay pairs. For example, the GPCR aminergic cluster (green) included several adrenergic GPCRs (rAdra1A/B, rAdra1/2_NonSelective, hAdrb1/2, hAdra2A/C, and rmAdra2B) and corresponding transporters (hNET) and also included several dopaminergic GPCRs (hDRD1, hDRD2s, hDRD4.4, and bDR_NonSelective) and their corresponding transporters (hDAT and gDAT). This implies a degree of consistency and specificity to the chemical biology of the perturbation. The kinase and phosphatase cluster (blue) was highly enriched with these assays and also included a phosphodiesterase (PDE4A1) and class-III HDAC (SIRT2). The largest nuclear receptor cluster (yellow) contained 8 assays (386 chemical–assay actives) all within subfamily 3, the steroid receptors (GR, AR, PR, and ER). Many of these assays were also among the most promiscuous (see Table 3).

3.3. Chemical Class Clusters. **3.3.1. Pesticides.** Pesticide active compounds, a main component of the ToxCast Phase I testing due to the availability of *in vivo* data, are designed to be biologically active in target species (i.e., insects, weeds, and fungi), while producing minimal effects on human biology. A diverse set of 470 pesticides in the combined Phase I and Phase II library considered here affected a large number of assays (236, 71%). Roughly 20% (105) affected no assays, whereas 41% (195) were included among the most promiscuous clusters (indicated by the top green and blue colored tree structures (Figure 1A) containing a total of 315 chemicals). The top active assays affected by pesticides included human

Table 4. Potent Chemical–Assay Pairs with AC50s at the Lowest Dose Tested^a

chemical name	AC50s		assay target(s)	refs
	total	LCT ^b		
chlorpromazine hydrochloride	55	7	TR_hNET, GPCR_hDRD1/2s, pSHT2C, hH1, rAdra1A/1B	55–58
haloperidol	42	6	OR_gSIGMA_NonSelective, GPCR_hDRD1/2s/4.4, GPCR_rAdra1_NonSelective, GPCR_bDR_NonSelective	59–61
trelanserin (SL650472 pharma)	24	6	GPCR_h5HT2A/7, pSHT2C, rSHT_NonSelective, GPCR_hDRD1/4.4	62
17 β -estradiol	9	5	NR_hAR, bPR, mERa, hER, bER	63,64
17 α -ethinylestradiol	24	4	NR_hAR, mERa, hER, bER	65
CP-471358 pharma	6	3	ENZ_hMMP13/2/9	66
CP-544439 pharma	10	3	ENZ_hMMP13/2/9	67
diethylstilbestrol	31	3	NR_mERa, hER, bER	68
2,2-bis(4-hydroxyphenyl)-1,1,1-trichloroethane	36	3	NR_mERa, bER, hCAR_Antagonist	69
zamifenacin (pharma)	60	3	GPCR_gMPeripheral_NonSelective, hM3/5	70,71
flufenacet	10	2	MP_rPBR, NR_hPXR	
maneb	62	2	ENZ_hPTPN9/4	
methadone hydrochloride	37	2	GPCR_rOpiate_NonSelective/Na	72
progesterone	11	2	NR_hAR, NR_bPR	73
SR144190 pharma	24	2	GPCR_hNK2, NR_hPXR	74
tetraconazole	24	1	ADME_hCYP2C19	
diniconazole	5	1	ADME_hCYP2C19	
flufenpyr-ethyl	2	1	ADME_hCYP4F12_Activator	
tannic acid	26	1	ENZ_hGSK3b	75
chlorpyrifos oxon	14	1	ENZ_hES	76
mancozeb	88	1	ENZ_hDUSP3	
CP-105696 pharma	5	1	GPCR_gLTB4	77
diphenhydramine hydrochloride	41	1	GPCR_hH1	78
elzasonan (CP-448187 pharma)	5	1	GPCR_hAdrb2	
emamectin benzoate	65	1	GPCR_hNTS	
disodium (5S,6R,7R)-5-(1,3-benzodioxol-5-yl)-2-butyl-7-{2-[(2S)-2-carboxylatopropyl]-4-methoxyphenyl}-6,7-dihydro-5H-cyclopenta[b]pyridine-6-carboxylate (pharma)	7	1	GPCR_hETA	
PHA-00543613 pharma	12	1	LGIC_rNNR_BungSens	79
CP-457920 pharma	2	1	LGIC_bGABARa5	80
2,6-difluoro-5-[3-(2-hydroxypropan-2-yl)imidazo[1,2-b][1,2,4]triazin-7-yl]biphenyl-2-carbonitrile (pharma)	4	1	LGIC_bGABARa5	81
sodium 3-(4-{[1-(3-ethoxyphenyl)-2-(4-methylphenyl)-1H-imidazol-4-yl]carbonyl}piperazin-1-yl)naphthalene-1-carboxylate (pharma)	31	1	GPCR_mCCKAPeripheral	82
CP-122721 pharma	44	1	GPCR_rNK1	83
SAR102779 pharma	43	1	GPCR_hNK2	84
SSR241586 pharma	66	1	GPCR_rNK3	85
SAR150640 pharma	53	1	GPCR_hDRD2s	86
SSR103800 pharma	33	1	GPCR_gOpiateK	
enadoline (pharma)	6	1	GPCR_gOpiateK	87
SSR125047 pharma	59	1	OR_gSIGMA_NonSelective	88
spiroxamine	18	1	OR_gSIGMA_NonSelective	
4-(3-{[4-(2-methyl-1H-imidazol-1-yl)phenyl]sulfanyl}phenyl)tetrahydro-2H-pyran-4-carboxamide methanesulfonate (pharma)	19	1	TR_gDAT	
1-[2-(3,4-dichlorophenoxy)-5-fluorophenyl]-N-methylmethanamine (pharma)	11	1	TR_rSERT	89
UK-416244 pharma	43	1	TR_rSERT	90
6-{2-[4-(1,2-benzothiazol-3-yl)piperazin-1-yl]ethyl}-4,4,8-trimethyl-3,4-dihydroquinolin-2(1H)-one methanesulfonate (pharma)	9	1	GPCR_p5HT2C	
SB243213A pharma	8	1	GPCR_p5HT2C	91
volinanserin (pharma)	41	1	GPCR_h5HT2A	92
bisphenol B	31	1	NR_mERa	93
5,5-diphenylhydantoin	2	1	NR_hPXR	94
fenamiphos	5	1	NR_hPXR	
imazamox	2	1	NR_hPXR	
napropamide	14	1	NR_hPXR	
pyraclostrobin	9	1	NR_hPXR	
sodium hexyldecyl sulfate	29	1	NR_hPXR	
sorbitan	7	1	NR_hPXR	

Table 4. continued

chemical name	AC50s		assay target(s)	refs
	total	LCT ^b		
PK11195	21	1	MP_hPBR	95
zoxamide	2	1	MP_rPBR	

^aColumns indicate chemicals with AC50s at the lowest dose tested, the total number of calculated AC50s for the given chemical, the number of AC50s at the lowest dose (i.e., number of assays affected at the lowest dose), the assay target(s) with AC50 values at the lowest dose tested, and the literature evidence of the chemical–target interaction, if applicable. ^bLCT: lowest concentration tested.

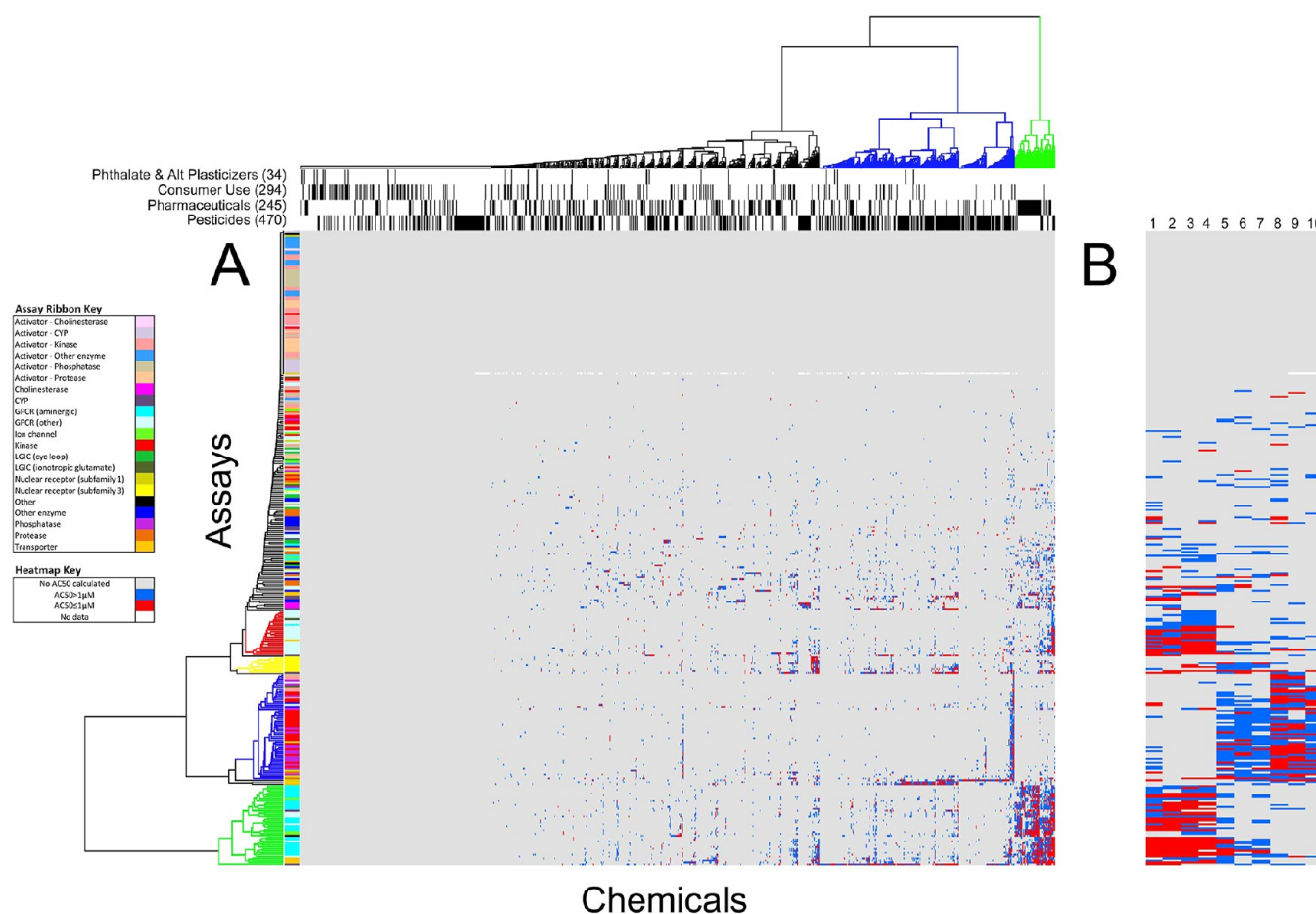


Figure 1. Hierarchical clustering of 976 chemicals by 331 biochemical assays. Hierarchical clustering was based on chemical–assay potency as measured by the inverse log of AC50s (in micromolar) divided by 1,000,000 ($-\log(\text{AC50}/1000000)$). Actives with AC50 values $\leq 1 \mu\text{M}$ are colored red and others blue. Gray indicates inactive and white not tested in Phase I (hCAR_Agonist assay). (A) Left ribbon indicates clusters of 21 assay categories (see Assay Ribbon Key). Left colored tree structure indicates relatively homogeneous assay category clustering including GPCR (other), red; nuclear receptor (subfamily 3), yellow; kinases and phosphatases, blue; GPCR (aminergic), green. Top bars indicate clusters of 4 chemical use groups. Top colored tree structure indicates highly promiscuous, mostly pharmaceuticals (green) and promiscuous, mostly pesticides (blue). (B) Details for 10 of the most promiscuous chemicals listed in Table 2. Heavy metals (1-phenylmercuric acetate, 2-mercuric chloride, 3-tributyltin methacrylate, 4-tributyltin chloride); surfactants (5-sodium dodecylbenzenesulfonate, 6-perfluorooctane sulfonic acid, and 7-dodecylbenzene sulfonate triethanolamine (1:1)); and dithiocarbamate fungicides (8-mancozeb, 9-maneb, and 10-metiram).

CYP2C19, CYP2C9, CYP1A2, and CYP2B6 enzymatic inhibition assays (165, 79, 74, and 55 chemicals, respectively), human PXR binding assay (116), and rat and human TSPO binding assays (104 and 74). Examples of chemical–assay actives are highlighted for their known chemical–target interactions. Carbofuran, an insecticide known to inhibit cholinesterase, inhibited only 3 assays: butyrylcholinesterase and, at submicromolar AC50 concentrations, the human and rat acetylcholinesterase enzymatic assays. Picoxystrobin, a strobilurin fungicide that inhibits fungal respiration, affected only 4 assays, including the human CYP2C9 and CYP2C19 enzyme assays, as well as the human TSPO and, at submicromolar

AC50 concentrations, the rat TSPO enzymatic assay. Two other members of the strobilurin class of fungicides, described in the previous Phase I analysis,⁹ also affected a small number of assays (3–9), including TSPO. Hence, for a number of examples, the activity displayed in this biochemical platform for selected pesticides reflected bioactivities associated with their known pesticidal modes of action and/or potentially related targets.

3.3.2. Pharmaceuticals. Pharmaceuticals (245), including the 111 donated compounds, are intended for biologic activity like pesticides but toward mammalian biology. The pharmaceuticals are also more likely to have a defined target. There

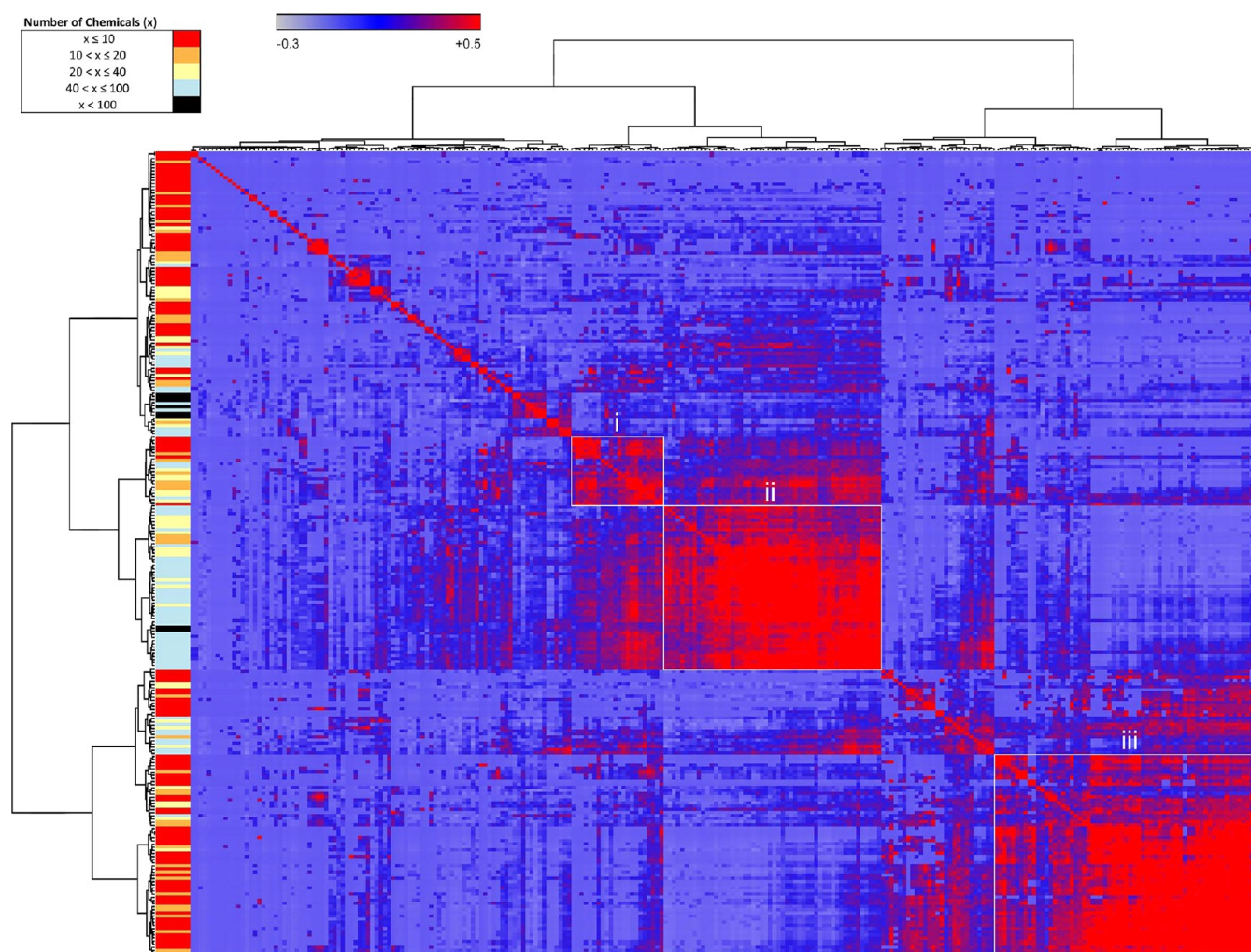


Figure 2. Assay–assay similarity matrix clustered based on chemical–assay profiles. Pearson correlations (–0.3 to 0.5) indicated the strength of associations, which were visualized in the heatmap from blue to red, respectively. Similar assays clustered along the diagonal have high associations. Selected clusters (i, ii, and iii) are shown as examples and listed in Table 5. The left color bar indicates the number of chemicals affecting a given assay.

were 36 pharmaceuticals that did not produce an AC50 for any of the target assays tested here; however, 37 pharmaceuticals clustered tightly by inhibition of GPCR binding activities (Figure 1A).

Several examples could be found to indicate chemical–assay actives for known chemical–target interactions. For example, volinanserin, a serotonin receptor antagonist,²⁵ inhibited 41 different assays, the majority of which were GPCRs and transporters (78%), including the serotonergic system (affecting 9 out of 11 total serotonergic assays) (see Supporting Information, Table S2). Several examples could be found to indicate chemical–assay actives for unknown chemical–target interactions. For example, anthralin is a topical antiproliferative, anti-inflammatory agent used to treat psoriasis;²⁶ however, the mechanisms of action are unknown. Anthralin inhibited 22 assays, almost exclusively enzymes, including caspases 1–5 and 8 (where the inflammatory caspase 5 activity was inhibited at submicromolar AC50 concentrations), MMPs 1/2/3/7/13, and cyclooxygenases PTGS1/COX1 and PTGS2/COX2 (see Supporting Information, Table S2). These data indicate that the biochemical activity profiles of pharmaceuticals provide information on potential novel effects in addition to their

known activities, giving possible leads for further targeted studies.

3.3.3. Consumer Use Chemicals. Consumer use chemicals tested here (171), exclusive of pesticides and pharmaceuticals that were described above, showed spotted activity based on the number of targets affected across the assay space (42% of this chemical class) or, in some cases, were highly promiscuous (9% of this chemical class) (Figure 1A). Example chemicals in this class include food additives and ingredients in sunscreens, cosmetics, soaps, and shampoos. Of the chemicals showing activity (100), the median number of assays affected per chemical was 2, with a range of 1 to 72 assays. Consider caffeine as an example. Caffeine is a known adenosine receptor antagonist. Caffeine and the structurally related methylxanthine, theophylline, inhibited all three adenosine receptor binding assays (hAdo2a, hAdo1, and nonselective bAdo receptor). Interestingly, adenosine receptor binding activities were also inhibited by the 2'-deoxyadenosine analogue, cladribine, an effect recently reported.²⁷ The 13 perfluorinated compounds, which are industrial and consumer use products (e.g., surfactants and nonstick applications), showed a wide range of chemical-specific activity (median 6 assays). For example, 1,1,2,2-tetrahydroperfluoro-1-decanol inhibited none of the

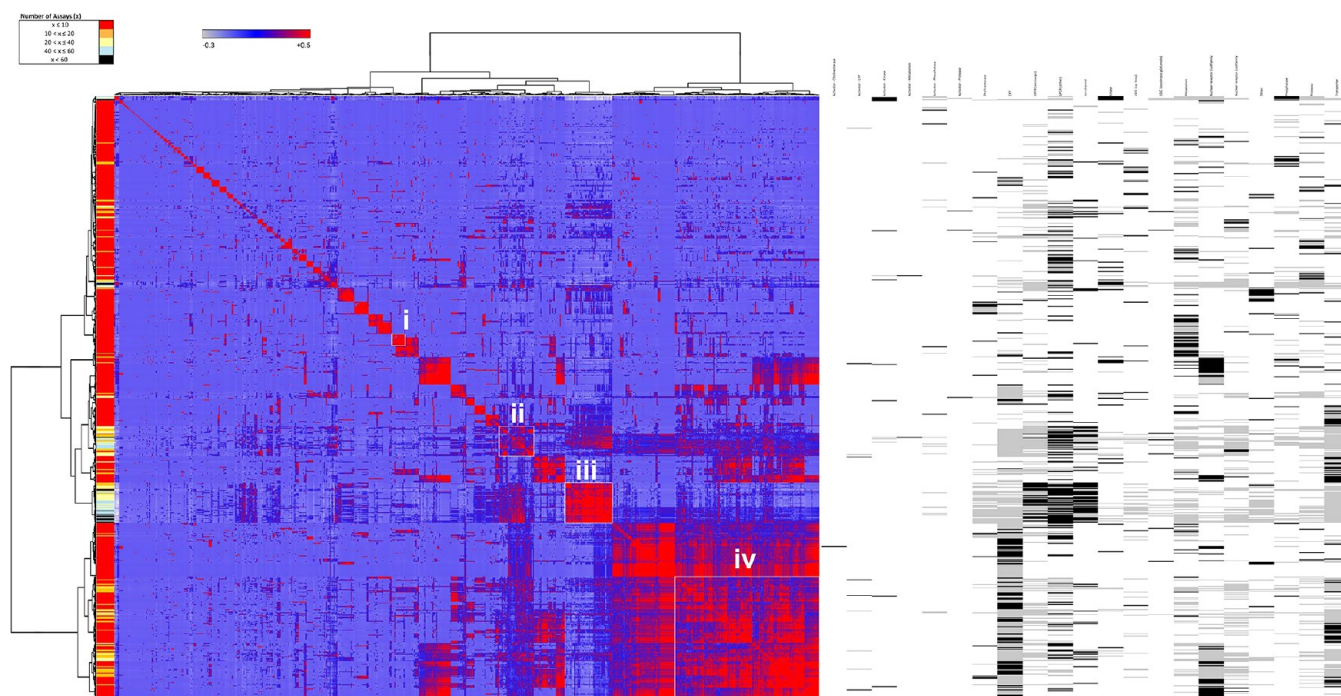


Figure 3. Chemical–chemical similarity matrix clustered based on chemical–assay profiles. Pearson correlations (-0.3 to 0.5) indicated the strength of associations, which were visualized in the heatmap from blue to red, respectively. Similar chemicals clustered along the diagonal have high associations. Selected clusters (i, ii, iii, and iv) are shown as examples and listed in Table 6. The left color bar indicates the number of assays affected by a given chemical. The right panel indicates the assay enrichment scores (defined in the Experimental Procedures section) for each chemical and can be used to describe the chemicals in the clusters.

assays, whereas perfluorooctane sulfonic acid (PFOS) inhibited 72 assays. Across all perfluorinated compounds, the most commonly affected assay (inhibited by 10 of 13 chemicals) was the leukotriene B4 (GPCR_gLTB4). Other leukotriene assays (GPCR_hLTB4_BLT1, gLTD4) were inhibited by 30% (4) of the perfluorinated compounds. Although these data indicate that most chemicals labeled for consumer use in the ToxCast library, excluding pesticides, were generally inactive in the biochemical HTS platform, there are case examples where some broad use categories are active against particular assay categories.

3.3.4. Phthalate Plasticizers and Alternatives. There is evidence that phthalate plasticizers are endocrine active.²⁸ Alternatives to phthalate plasticizers have been proposed to eliminate this undesired effect,²⁹ however, many alternatives have not undergone rigorous testing.³⁰ Thirty-four plasticizers, including 7 phthalates and 27 potential alternatives, were tested here. Overall, 12 plasticizers were inactive across all 331 assays (see Figure 1A). These included 1 phthalate and 11 nonphthalate alternatives. Of the remaining 22 compounds, 15 were active in 1 to 2 assays (3 phthalates and 12 nonphthalates), and 7 were active in 3 to 6 assays (3 phthalates and 4 nonphthalates). The most frequent assay targets for these compounds were CYPs (CYP2C19 and CYP1A2) and TSPO (human and rat). Only two plasticizers inhibited any nuclear receptor binding and only at higher concentrations (DEHP inhibited hGR at an $AC_{50} = 95 \mu\text{M}$, and diethyl succinate inhibited rMR at an $AC_{50} = 49 \mu\text{M}$; see Supporting Information, Table S2). Limited phthalate and estrogen receptor binding is not surprising, given that half-maximal inhibitory concentrations for binding have been reported to be $1000 \mu\text{M}$.³¹ No statistical difference ($p > 0.05$ from t test)

between the responses of the phthalate and nonphthalate plasticizers to these particular assays could be concluded.

3.4. Assay and Chemical Similarity Matrices. To evaluate the similarities among assays (Figure 2) and chemicals (Figure 3), we performed Pearson's correlation based on chemical–assay activities. Assays or chemicals that are most associated together cluster as blocks along the diagonal. Nonoverlapping clusters of assays (Figure 2) or chemicals (Figure 3) with positive Pearson's correlations are shown as examples. The left-hand ribbon indicates the number of chemicals active in an assay (Figure 2) or assays active for a given chemical (Figure 3). A caveat of this correlation model is that the size of a cluster may be driven by one to two assays in the chemical similarity matrix or one or two chemicals in the assay similarity matrix.

3.4.1. Evaluation of Assay Similarities. Assay–assay similarity was performed over the 256 active assays (Figure 2). The basis for highly similar clusters (Pearson's correlation ≥ 0.65) in some cases was associated with a specific response to relatively few chemicals, such as the case with the human caspases 1–3 (active for 5–9 chemicals) and histone deacetylases 3 and 6 (active for 5–8 chemicals). In other cases, high-similarity clustering was driven by a large number of chemicals causing activity in related assays, such as that seen with TSPOs (inhibited by 117–147 chemicals), acetylcholinesterases (41–46 chemicals), and estrogen receptors (18–30 chemicals). Three other clusters are highlighted in Figure 2 and Table 6 to demonstrate the composition of a cluster that aggregated due to chemical–assay response similarity. Cluster i holds 22 assays perturbed by 2 to 64 chemicals. These were mainly GPCR_other assays (18). Two subclusters (non-overlapping clusters with Pearson's correlation ≥ 0.65) within Cluster i each contain peptide GPCRs, including glutamate,

Table 5. Known Estrogenic and Nonestrogenic Compounds^a

relative potency	chemical name	AC50s (μM)		
		bER	hER	mERa
inactive	atrazine	0	0	0
inactive	linuron	0	0	0
inactive	haloperidol	0	0	0
inactive	phenobarbital sodium salt	0	0	0
inactive	progesterone	0	0	0
inactive	ketoconazole	0	0	0
	<i>inactive summary</i>	100%	100%	100%
very weak	ethylparaben	0	0	0
very weak	methoxychlor	0	0	0
very weak	butyl benzyl phthalate	0	0	0
	<i>very weak summary</i>	0%	0%	0%
weak	4-(1,1,3,3-tetramethylbutyl)phenol	33.000	7.200	8.200
weak	kepone	0	0	0
weak	genistein	0.130	0.032	0.130
weak	4-cumylphenol	16.000	0	12.000
weak	bisphenol B	0.430	0.300	0.023
weak	<i>o,p</i> -DDT	0	0	0
weak	bisphenol A	0.630	0.820	1.100
weak	4-nonylphenol, branched	33.000	20.000	5.600
weak	butylparaben	56.999	17.000	23.000
	<i>weak summary</i>	78%	67%	78%
strong	17 β -estradiol	0.023	0.023	0.023
strong	diethylstilbestrol	0.023	0.023	0.023
strong	17 α -ethinylestradiol	0.023	0.023	0.023
	<i>strong summary</i>	100%	100%	100%
antagonist	tamoxifen	0.100	0.330	0.200
	<i>antagonist summary</i>	100%	100%	100%

^aThe chemicals are listed along with their relative potency for the estrogen receptor (as noted within the EPA's Endocrine Disruptor Screening Program) and calculated AC50 values for the three estrogen assays. The summary for each potency category indicates the percent of chemical-AC50 combinations that were correctly identified in the HTS.

vasoactive intestinal peptide, endothelin, and angiotensin II GPCRs, as well as the neuropeptide Y GPCRs. Cluster ii involves 52 assays active for 16 to 136 chemicals. The assays were mainly within the GPCR_aminergic (32), GPCR_other (7), and transporter (6) categories. One subcluster contained rhodopsin-like biogenic amine GPCRs, including histamine, muscarinic acetylcholine, adrenergic, serotonergic, and dopaminergic GPCRs, another containing three opiate GPCRs, and the third containing two ion channels. Cluster iii involves 41 assays active for 2 to 41 chemicals. The assays represented were mainly within the kinase (21) and phosphatase (14) categories. Both subclusters included relatively equal numbers of kinases and class I cysteine-based protein tyrosine phosphatases; however, the kinases were distinct for each subcluster with tyrosine and CAM kinases in one and mainly tyrosine kinases in the other. The assay similarities revealed clusters of targets known to be similar (e.g., GPCRs), as well as varied or dissimilar targets. These findings demonstrate a biological basis to clustering of chemicals in the assay similarity matrix.

3.4.2. Evaluation of Chemical Similarities. Clustering by chemical-chemical similarity was performed on 729 active chemicals (Figure 3). There are 55 such clusters (>65% similar) based on a small number of assays (<4) that range in size from

Table 6. Assay-Assay Similarities^a

clusters ^b	assay categories ^c	assay targets
		Cluster i (22)
subcluster1	GPCR (other) (4)	<i>rmMgluR5</i> , <i>rVIP</i> (nonselective), <i>hETB</i> , <i>bAT2</i>
subcluster2	GPCR (other) (2)	<i>hNPY2</i> , <i>bNPY</i> (nonselective)
		Cluster ii (52)
subcluster1	GPCR (aminergic) (18)	<i>hH1</i> , <i>gH2</i> , <i>hM1-5</i> , <i>gMperipheral</i> , <i>rAdra1A&B</i> , <i>rAdra1&2</i> (nonselective), <i>hAdra2A</i> , <i>rmAdra2B</i> , <i>hAdrb2</i> , <i>rSHT</i> (nonselective), <i>hSHT2A</i> , <i>bDR</i> (nonselective)
	GPCR (other) (3)	<i>gOpiateK</i> , <i>rOpiate Non-Selective</i>
	ion channel (2)	<i>rNaCh</i> , <i>rCaBTZCHL</i>
subcluster2	GPCR (aminergic) (7)	<i>hDRD1</i> , <i>hDRD2s</i> , <i>hDRD4.4</i> , <i>hSHT5A</i> , <i>hSHT7</i> , <i>hAdra2C</i> , <i>hAdrb1</i>
	GPCR (other) (2)	<i>hOpiateD1 & Mu</i>
		Cluster iii (41)
subcluster1	activator: kinase (4)	<i>hNEK2</i> , <i>hFyn</i> , <i>hIGF1R</i> , <i>hSRC</i>
	kinase (3)	<i>hMAPKAP2</i> , <i>hMAPK3</i> , <i>hPAK4</i>
	activator: phosphatase (1)	<i>hPPM1A</i>
	phosphatase (4)	<i>hPTPN4</i> , 9, 14, <i>hACP1</i>
subcluster2	kinase (9)	<i>hRAF1</i> , <i>hCSF1R</i> , <i>hEGFR</i> , <i>hMAPK1</i> , <i>hTie2</i> , <i>hMsk1</i> , <i>hVEGFR2&3</i> , <i>hAurA</i>
	phosphatase (7)	<i>hPTPN1</i> , 2, 6, 11, 12, <i>hPTPRB</i> , <i>hPTEN</i>

^aThree clusters were identified through assay similarity analysis for further analysis. ^bSubclusters were identified from clusters along the diagonal with $\geq 65\%$ similarity. Numbers in parentheses indicate the number of assays within a cluster. ^cNumbers in parentheses indicate the number of assays within an assay category.

2 to 17 chemicals. Some examples include a cluster of 17 chemicals active in only the CYP2C19 assay and a cluster of 14 chemicals active in only the human PXR assay. Other clusters are driven by a few promiscuous chemicals, such as the cluster containing maneb, mancozeb, and metiram, and another cluster containing surfactants such as sodium dodecyl sulfate and PFOS. Smaller clusters with chemicals active in a limited number of assays revealed specificity within the data set: α -cyclodextrin, 17 β -estradiol, and genistein (active in 5–9 assays) inhibited the three estrogen assays; two compounds CP-544439 and CP-471358 (active in 6–7 assays) inhibited MMPs 1/2/3/9/13, as well as the leukotriene B4 GPCR; rifampicin and *tert*-butylhydroquinone (active in 6–7 assays) inhibited PTGS1/COX1 and PTGS2/COX2 enzymatic activities, as well as CYP2C9 and CYP2C19; and eight chemicals (caffeine, theophylline, cladribine, cyanazine, triflurosulfuron-methyl, and prometryn, active in 3–9 assays) inhibited three human adenosine A receptors A1.

Four other clusters are highlighted in Figure 3 and Table 7 to demonstrate the substructure of a cluster that aggregated due to chemical-assay response similarity. To describe the clustered chemicals in terms of activity in the 21 assay categories, we used an enrichment score for each chemical (Figure 3, right panel). This chemical-assay category score indicates specificity of a chemical to affect assays within a given assay category over other categories. Cluster i has 29 chemicals active in 1 to 19 assays, enriched for Other enzyme. The subclusters include 1-

Table 7. Chemical–Chemical Similarities^a

clusters ^b	chemical name ^c
enriched assay group	Cluster i (29)
subcluster1	other enzyme (29)
subcluster2	1-[<i>cis</i> -1-(3-ethoxyphenyl)-4-methylcyclohexyl]-4-phenylpiperazine methanesulfonate (1:1) (pharma); coumarin; DTBP; pioglitazone hydrochloride 2,4-DNT; 2,3-DNT; 2,6-DNT; 2,4,5-trichlorophenol; DNB; Michlers ketone; 4-nitrophenol; dichlobenil; 4-chloro-3-methylphenol; 3-((3R,4R)-6-[(5-fluoro-1,3-benzothiazol-2-yl)methoxy]-4-hydroxy-3,4-dihydro-2H-chromen-3-yl)methyl)benzoic acid (pharma)
enriched assay group	Cluster ii (36)
subcluster1	GPCR (other) (33), ion channel (26), CYP (33), GPCR (aminergic) (32), nuclear receptor (subfamily 3) (31), transporter (33), other enzyme (22)
subcluster2	4-dodecylbenzenesulfonic acid; docusate sodium
subcluster3	4,4'-sulfonylbis[2-(prop-2-en-1-yl)phenol]; dorphene
subcluster4	bisphenol A; bisphenol B androstenedione; progesterone
enriched assay group	Cluster iii (49)
subcluster1	GPCR (aminergic) (49), GPCR (other) (47), ion channel (47), transporter (46), dolinesterase (38), CYP (36), other (34), other enzyme (27)
subcluster2	1,3-diphenylguanidine; spiroxamine; CP-728663 (pharma); 1,3-dichloro-6,7,8,9,10,12-hexahydroazepino[2,1-b]quinazoline hydrochloride (1:1) (pharma)
subcluster3	tributyltin chloride; tributyltin methacrylate methadone hydrochloride; volinaserin (pharma); haloperidol; diphenhydramine hydrochloride; SSR125047 (pharma); pentamidine isethionate; AVE8488 (pharma); SR271425 (pharma); SR236057A (pharma); GSK163929B (pharma); SSR240612 (pharma); UK-416244 (pharma); SARI02779 (pharma); SARI0640 (pharma); chlorpromazine hydrochloride; SSR150106 (pharma); zanfena (pharma)
subcluster4	phenylmercuric acetate; mercuric chloride
subcluster5	amidarone hydrochloride; (1R)-1-[(ethoxycarbonyloxy)ethyl]-1-[(5-(5-chlorothiophen-2-yl)-1,2-oxazol-3-yl)methyl]-2-[[1-(propan-2-yl)piperidin-4-yl]carbamoyl]-1H-indole-5-carboxylate hydrochloride (pharma); didecylidimethylammonium chloride; [4-(5-(aminomethyl)-2-fluorophenyl)piperidin-1-yl](4-bromo-3-methyl-5-propoxythiophen-2-yl)methanone hydrochloride (pharma); 5-(benzylsulfonyl)-2-[[2-(dimethylamino)ethyl](ethyl)amino]-N,N-dichloro-4-(4-phenylpiperidin-1-yl)benzamide (pharma); gentian violet; [4-[3-(aminomethyl)phenyl]piperidin-1-yl]{{S-[(2-fluorophenyl)ethyl]furan-2-yl}methanone (pharma)
enriched assay group	Cluster iv (149)
subcluster1	CYP (149), transporter (111), nuclear receptor (subfamily 1) (81)
subcluster2	rifampicin; tert-Butylhydroquinone
subcluster3	decane; doxtriazole; cyproconazole; fenbuconazole
subcluster4	3,3',5,5'-tetrabromobisphenol A; methoxychlor; paclobutrazol; triticonazole; fipronil; dimethoxane
subcluster5	2,5-ditert-butylbenzene-1,4-diol; Phenothiazine
subcluster6	CP-456773 (pharma); O-ethyl O-(4-nitrophenyl) phenylphosphonothioate metolachlor; chlorpyrifos-methyl; 2-(4-fluorophenoxy)-N-[4-(2-hydroxypropan-2-yl)benzyl]pyridine-3-carboxamide (pharma); DEHP; acetochlor; trifloxystrobin; fenpropathrin; disulfiram; chlorobenzilate; benodanil; 4,4'-methylenebis(2-methylamine); 6-chloro-2-phenyl-8,8a-dihydro-3aH-indeno[1,2-d][1,3]thiazol-3a-ol (pharma); butyl benzyl phthalate; 7,12-dimethylbenz(a)anthracene; dibutyl phthalate; triphenyl phosphite; dipropylene glycol dibenzoate; norflurazon; carfenazine-ethyl; rotenone; 3-pyridinylcarboxamide, 2-(2,1,3-benzoxadiazol-5-yl)-N-[[4-(1-hydroxy-1-methylethyl)phenyl]methyl] (pharma); picoxystrobin; fenoxycarb

^aFour clusters were identified through chemical similarity analysis for further analysis. The chemicals within each cluster were enriched for a number of assay categories, with the most associated in bold. Numbers in parentheses indicate the number of chemicals within the cluster and associated with the assay category. ^bSubclusters were identified from clusters along the diagonal with $\geq 65\%$ similarity.

^cChemicals within each subcluster are listed.

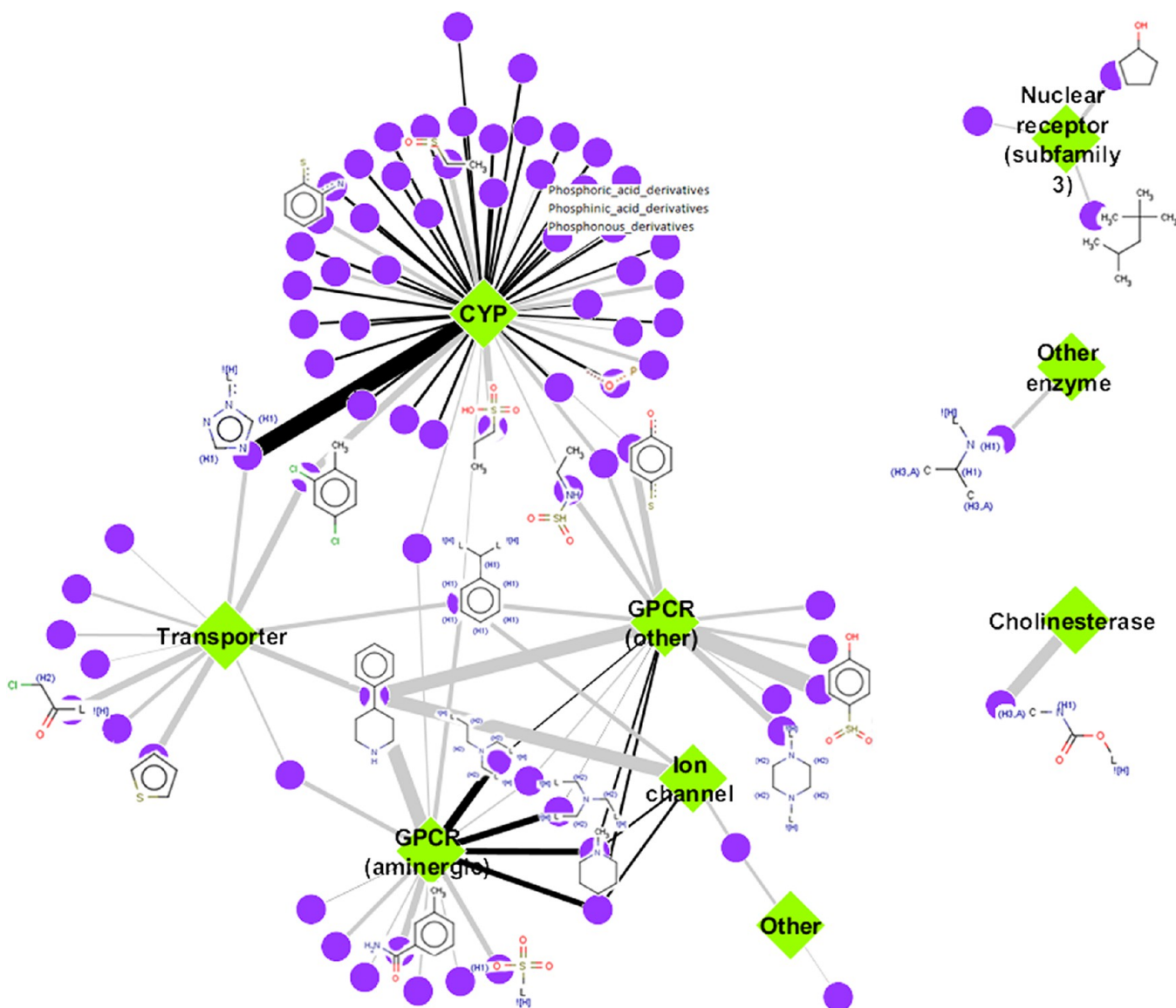


Figure 4. Chemical fragment–assay category associations. Univariate associations between chemical-structure fragments and enrichment scores for chemical–assay categories were performed to identify chemical fragments in chemicals specifically enriched for affecting an assay category. Chemical fragment–assay categories with true positives ≥ 5 and positive predictive value (PPV) >0.5 are visualized. Purple nodes are the chemical fragments, and green diamonds are the assay categories. Example chemical fragment structures are shown for the associations with the highest PPV (indicated by increasing edge thickness). Numbers of true positives are indicated by edge color from gray (5–9) to black (10–26).

[*cis*-1-(3-ethoxyphenyl)-4-methylcyclohexyl]-4-phenylpiperazine methanesulfonate (1:1) (pharma), coumarin, DTBP, pioglitazone hydrochlorine, a number of nitrotoluene and phenol compounds, Michler's ketone, dichlobenil, and 3-((3*R*,4*R*)-6-[(5-fluoro-1,3-benzothiazol-2-yl)methoxy]-4-hydroxy-3,4-dihydro-2*H*-chromen-3-yl)methyl)benzoic acid (pharma). Cluster ii includes 36 chemicals active in 7 to 65 assays, mostly enriched with GPCR (other) and ion channel assays, and includes five other assay enrichment categories. Four subclusters include two chemicals in each group. Subcluster1 includes 4-dodecylbenzenesulfonic acid and docusate sodium and is mostly enriched for the GPCR (other) assay category, whereas the other three subclusters are enriched for the nuclear receptor (subfamily3) category and includes subcluster2, with 4,4'-sulfonylbis[2-(prop-2-en-1-yl)-phenol] and chlorophene; subcluster3, with bisphenol A and B; and subcluster4, with progesterone and androstenedione.

Cluster iii involves 49 chemicals active in 12 to 90 assays, mostly enriched for GPCRs (both categories) and ion channels, as well as five others. Five subclusters were identified, including two subclusters with the most promiscuous chemicals, tributyltin chloride and tributyltin methacrylate, and phenylmercuric acetate and mercuric chloride. The other three clusters include at least half of the pharmaceuticals, most likely in the GPCR assay cluster from Figure 2. Cluster iv involves 149 chemicals active in 2 to 48 assays, enriched for CYPs, transporters, and nuclear receptor (subfamily 1). Many subfamilies were identified, but six were listed and contain mostly pesticides. The other subfamilies not listed were almost exclusively pesticides from Phase I of testing and discussed previously.⁹ The chemical similarities revealed known assay clusters (e.g., for bisphenols or heavy metal compounds) and previously unreported clusters (e.g., for pharmaceuticals).

These findings demonstrate a structural basis to clustering of assays in the chemical similarity matrix.

3.5. Common Chemical Structure Features Enriched for Specific Assay Categories. From the chemical activity similarity cluster, enriched assay categories can be identified. In turn, evaluating similar chemical structure fragments enriched in the assay categories can help describe the types of chemicals that are clustering together (Figure 4). Univariate analyses linking chemical structure fragments to assay categories (based on AC50s $\geq 10 \mu\text{M}$) revealed 107 associations for 84 unique chemical fragments and 9 assay categories. CYPs had the most associated chemical fragments, with a majority being subfragments involving phosphoric acid, phosphinic acid, and phosphonous derivatives; however, 1,2,4-triazole had the highest PPV. A benzene ring with two constituents and 4-phenylpiperidine were structures shared by the CYPs, transporters, GPCRs, and ion channel categories. Additionally, variations of the benzene ring were seen throughout the associations. Three assay categories that did not share chemical structures with other categories included NR_subfamily3_steroid associated with cyclopentanol and 2,2,4-trimethylpentane; the other enzyme category associated with isopropylamine; and cholinesterase associated with *N*-methylcarbamate. Overall, the chemical fragments from chemicals in this data set that are enriched for affecting an assay category are generally unique, but overlap is observed.

4. DISCUSSION

The data set analyzed here profiles 976 structurally and categorically diverse chemicals in the ToxCast library across 331 biological assays. These data were derived from two temporally separated testing phases: (1) 310 unique chemicals analyzed across 292 assays from the original Phase I v1 of ToxCast, reanalyzed using an improved algorithm for automated curve-fitting across 230 assays retained in Phase II; and (2) new data generated for 676 unique structures (including 9 Phase I compounds in replicate) in Phase II analyzed across 231 assays. In total, the combined set provides bioactivity data for 976 chemicals (Phase I, II) profiled across 331 assays (231 assays plus 100 analyzed for activation) for ligand–receptor binding and enzymatic activities. Patterns derived from these profiles can only be interpreted within the context of the specific assays covered here and do not imply *in vivo* toxicity or lack thereof since the biochemical screen does not consider kinetics and metabolism (ADME) and intra/intercellular signaling. Results from this study extend the previous analysis⁹ to a broader chemical landscape, revealing both major and minor patterns for groups of chemicals and biochemical assays.

Roughly a quarter of the 976 compounds tested showed no demonstrable activity (AC50) in any of the assays used herein, including many consumer use chemicals, phthalates, and green alternatives. The remaining compounds tested here showed specific or promiscuous activities. Clustering revealed coarse relationships by chemical use category, chemical structure, and/or biological target. For example, most pesticidal actives and pharmaceuticals could be resolved by target signatures, AChE and nuclear receptors on the one hand versus GPCRs and transporters on the other. A similar degree of promiscuity ascribed to the Phase I chemical library⁹ was also noted here for the broader chemical landscape. Perhaps surprisingly, 7 of the 20 most promiscuous compounds were pharmaceuticals. This promiscuity, directed across the GPCR assays, partly reflected

the large contingent of GPCR assays included in this screen but also suggests a potential for off-target effects. Inherent chemical factors such as surfactant or detergent properties and metal-based or metal-chelating properties could also account for promiscuity. In particular, the polymeric dithiocarbamate pesticides affected multiple kinase and phosphatase assays that require divalent cations (magnesium or manganese) and/or have active site cysteine residues sensitive to oxidation. This specific effect was noted previously for maneb, mancozeb, and metiram,⁹ consistent with a mechanism of action associated with the inhibition of metal-dependent and sulfhydryl enzymes,^{32,33} and seems to be specific to these compounds across the broader chemical landscape tested here. Lastly, compounds containing tin (e.g., tributyltin) and mercury (e.g., phenylmercuric acetate) broadly disrupted GPCR ligand-binding activities but not kinase or phosphatase activities. These examples suggest a systematic basis to the promiscuity and a degree of specificity to the biological target or assay conditions. Such systematic activity may be reflected in characteristic responses *in vivo*. For example, the promiscuous GPCR activity of the mercury-containing compounds is consistent with the neuropsychiatric effects seen in mercury poisoning, such as Minamata Disease or Mad Hatter Syndrome, whose symptoms include delirium and hallucinations, ataxia, numbness in hands and feet, general muscle weakness, narrowing of the field of vision, and damage to hearing and speech.^{34,35}

Biochemical profiling also identified previously unreported chemical–target interactions that may suggest potential modes of action or off-target effects. Anthralin, for example, is a topical drug used for treatment of psoriasis, but its mechanism of action is unknown. Consistent with the biology of psoriasis as an autoimmune skin disease,³⁶ anthralin specifically inhibited the activity of several protein targets that may play a role in inflammatory pathways (caspases, MMPs, and COX1 and 2). Tannic acid, which is known for inhibiting inflammatory processes,³⁷ also inhibited these protein targets. UK-416244, a selective serotonin reuptake inhibitor (SSRI) (<http://www.chemspider.com/Chemical-Structure.8123181.html>), inhibited the rat serotonin transporter (AC50 of $0.023 \mu\text{M}$) as expected but also showed moderate activity on GPCRs including the human and rat adrenergic receptors (AC50s of $0.29\text{--}12 \mu\text{M}$), which are known off-targets for SSRIs.⁵ The most common target of the perfluorinated compounds was the leukotriene B4 GPCR. Although this is not a known interaction, the interaction is plausible since leukotrienes are fatty acid signaling molecules, and perfluorinated compounds are hydrophobic and lipophilic. In addition, both chemicals and proteins are suggested players in immune function and may give clues to off-target effects.^{38,39}

Pharmaceuticals, of which 245 are included in this study, serve not only as an anchor for known interactions and off-target effects but also as a kernel for clustering environmental chemicals by potency, efficacy, and specificity. A similarity matrix clustering chemical compounds by their assay targets classified two triazine herbicides (cyanazine and prometryn) with caffeine, theophylline, and cladribine based on a relatively selective effect on human adenosine receptors. The latter three compounds are known (or suspected) to disrupt pathways in adenosine signaling or metabolism and may serve to anchor the potential activity of cyanazine or prometryn to adenosine signaling.

Co-clustering of biologically related assays is also useful in discovering potentially unknown interactions. Consider, for example, assay clusters for biogenic amine GPCRs and peptide GPCRs from the assay by assay similarity matrix. A number of chemical compounds preferentially affected these two GPCR subfamilies. In addition, the biogenic amine GPCRs had a closer relationship with the disruption of opiate GPCRs, transporters for norepinephrine, serotonin, and dopamine, and sodium or calcium channels. Consideration to the broader range of biochemical targets may be informative data to train structure models for predicting chemical–target interactions. The major and minor patterns of associations from the biochemical profiling can be used in conjunction with (or to inform) computational approaches, such as the structure–activity relationship or similarity ensemble approach analyses.^{5,40,41}

Additional analyses for discovering unknown interactions may come from the enrichment of common chemical fragments in association with specific or multiple assay targets. These chemical fragment associations suggest that if a new chemical contains this chemical fragment, it has a greater likelihood of affecting a given assay category and could provide clues governing chemical interactions for a specific or multiple assay targets. For example, phenol-containing compounds are well known to interact with the estrogen receptor (within the steroid subfamily 3 of nuclear receptors),⁴² but chemicals containing the phenol fragment were also associated with promiscuous inhibition of CYPs, thereby not specifically associating with the steroid subfamily 3 category. Similarly, organophosphates are known cholinesterase inhibitors for some insecticides, and chemicals containing this fragment were also associated with the inhibition of various CYPs and not specifically with cholinesterase inhibition. The cyclopentanol and 2,2,4-trimethylpentane fragments are inherent features of but not robust drivers of chemicals predicted to inhibit steroid receptor binding.⁴³ The gross association of fragments with assay enrichment in some cases and not others may provide a departure point for building more specific structure–activity relationship models, i.e., determining chemical property or feature modifiers that could potentially distinguish more specific activity subclasses within the fragment-containing clusters. However, examples of fragment–assay associations consistent with a priori knowledge include the association of an *N*-methylcarbamate fragment of some insecticides to anti-cholinesterase activity⁴⁴ and the isopropylamine fragment to some inhibitors of monoamine oxidases.⁴⁵ Beyond feature enrichment for certain chemical clusters (chemotyping), this biochemical HTS, together with nonbiochemical ToxCast assays and structure similarity, can serve as a broader resource for mapping structure–activity relationships to biological profiles and *in vivo* toxicities. The full range of the biochemical HTS could be used, for example, to test the hypothesis that structural analogues and/or chemicals sharing a common mechanistic category show sufficiently similar signals and whether or not such response signatures are specific enough to delineate a unique read-across grouping. Comparisons have been made between the Phase I chemical–assay effects and adverse outcomes, where a considerable amount of *in vivo* data is available.^{3,46,47} A challenge will be to address the clustering of Phase I and Phase II chemicals by biological response given the lack of *in vivo* data for most of the Phase II chemicals.

Biochemical inhibition of CYP activity may indicate a potential for the chemical to disrupt intermediary metabolism

in vivo or alternatively that the xenobiotic may be preferentially metabolized *in vivo*. Other specific interactions, either unrelated to cellular mechanisms or without obvious biological significance may be detected in the biochemical screen. For example, the soluble dietary fiber α -cyclodextrin inhibited all three estrogen assays (hER, mERa, and bER) and clustered with the known ER ligands estradiol and genistein. This interaction may be similar to that known for β -cyclodextrin through clathrate formation to sequester estrogen in a lattice.⁴⁸ Cyclodextrins are relatively nontoxic, however, due to their inability to penetrate lipophilic membranes.⁴⁹ Although these cell-free data may not always point to a biologically relevant process, the specificity of activity within a complex chemical–assay matrix may, nevertheless, provide useful information about the chemical compounds in their interaction with specific protein targets.

Since these chemicals were tested at or below 50 μ M, it may be difficult to extrapolate the current AC50 concentrations to *in vivo* activity since the concentrations are high relative to what might be achieved during *in vivo* exposure.⁵⁰ However, a number of chemical–assay pairs showed an AC50 at or below 1 μ M, which would seem attainable at least in high-dose testing animal studies. Along these lines, negative compounds that exhibit adverse outcomes *in vivo* could have been missed in the cell-free biochemical screen due to (a) bioavailability resulting in a xenobiotic metabolite not in the ToxCast chemical inventory; (b) the biological target not being represented, e.g., the 331 assays do not cover all possible targets; (c) the 50 μ M concentration not being high enough; or (d) the fact that the chemical–assay pair activity was not observed in the single screen due to assay variability, compound instability, or assay interference and hence not followed up by concentration–response. Furthermore, the concentration–response data is being made public with this article for user interpretation (<http://actor.epa.gov>). These points indicate areas for future research, specifically performing more extensive ADME analyses, consulting other cell-based assays for target validation and further expansion of the assay set, and identifying bioactivity signatures of broad chemical classes for which we could then query the toxicological space.

Moving forward, this large data set contributes significantly toward advancing new a regulatory paradigm through predictive toxicity and a better understanding of mechanisms.² The biochemical HTS screen offers preliminary evidence for chemical targets in a cell or tissue that, when combined with information from the literature or targeted studies, indicates potential pathways of toxicity. Predictive signatures developed from combinations of assays may be linked to an adverse outcome pathway.^{3,46,47,51,52} Efforts are underway to incorporate chemical features into these types of analyses to identify potential structural alerts that in combination with the HTS assays may be more predictive. These types of data and alerts can potentially provide biological predictions about chemicals with little to no biological information. In addition, *in silico* models are incorporating this information with cell–cell and tissue level behavior to predict outcomes of changing dose and time within a developing organ, without the need to pick up a pipet.⁵³

Overall, these results expand the ToxCast database to include a large and more structurally diverse set of chemicals. They also contribute to a novel framework for describing the interaction of environmental chemicals with important biochemical targets. By broadly surveying both the chemical landscape and

biological target space, patterns of biochemical activity have been identified which can help focus future research toward potential chemical–biological interactions that may result in adverse outcomes *in vivo*. The use of a quantitative approach in determining the potency of chemicals against each biological target, utilizing a diverse chemical library containing many reference chemicals with known activities as chemical probes, provides the context to better understand the potential for hazard of those chemicals with limited toxicity information. As these interactions become better defined through methods such as incorporation into adverse outcome pathways,^{7,54} these *in vitro* screening methods may ultimately serve as an efficient means of avoiding unwanted biological activity early in the chemical design and development process.

■ ASSOCIATED CONTENT

■ Supporting Information

All assays and assay descriptions; miniSOPs and curve fit figures linked to Table S1; and matrix of all chemical–assay AC50 values, in order as displayed in Figure 1. This material is available free of charge via the Internet at <http://pubs.acs.org>.

■ AUTHOR INFORMATION

Corresponding Author

*National Center for Computational Toxicology (B205-01), Office of Research & Development, U.S. Environmental Protection Agency, Research Triangle Park, NC 27711. (N.S.S.) Phone: 919 541 0103. Fax: 919 541 1194. E-mail: sipes.nisha@epa.gov. (T.B.K.) Phone: 919 541 9776. Fax: 919 541 1194. E-mail: knudsen.thomas@epa.gov.

Notes

The views expressed in this article are those of the authors and do not necessarily represent the views or policies of the U.S. Environmental Protection Agency. Mention of trade names or commercial products does not constitute endorsement or recommendation for use.

The authors declare no competing financial interest.

■ ACKNOWLEDGMENTS

We thank Mr. John Southerland for excellent management of EPA contracts with Caliper Discovery Alliances and Services, A PerkinElmer company and Evotec. Special thanks to the entire ToxCast team and pharmaceutical partners for their helpful insights. We also thank Dr. Scott Auerbach (NIEHS/NTP), Dr. Steve Simmons (EPA/NHEERL), and Dr. Mark Miller (EPA/OSP) for their valuable comments.

■ ABBREVIATIONS

AC50, half-maximal activity concentration; CYP, cytochrome P450; DMSO, dimethyl sulfoxide; DNT, dinitrotoluene; DTBP di-*tert*-butyl peroxide; ES enrichment score; GPCR, G-protein-coupled receptor; HTS high-throughput screening; LCT, lowest concentration tested; LGIC, ligand-gated ion channel; μ M, micromolar; mM, millimolar; M, molar; MAD2, 2.0 median absolute deviations from the median; MMP, metalloproteinase; NVS, NovaScreen panel; *p*, probability; PFOS, perfluorooctane sulfonic acid; PPV, positive predictive value; PXR, pregnane X receptor; QC, quality control; SDF, Structure Data Format; SSRI, selective serotonin reuptake inhibitor; TSPO, translocator protein

■ REFERENCES

- (1) NRC (2007) *Toxicity Testing in the 21st Century: A Vision and a Strategy*, National Academies Press, Washington, D.C.
- (2) Kavlock, R., Chandler, K., Houck, K., Hunter, S., Judson, R., Kleinstreuer, N., Knudsen, T., Martin, M., Padilla, S., Reif, D., Richard, A., Rotroff, D., Sipes, N., and Dix, D. (2012) Update on EPA's ToxCast program: providing high throughput decision support tools for chemical risk management. *Chem. Res. Toxicol.* 25, 1287–1302.
- (3) Judson, R. S., Houck, K. A., Kavlock, R. J., Knudsen, T. B., Martin, M. T., Mortensen, H. M., Reif, D. M., Rotroff, D. M., Shah, I., Richard, A. M., and Dix, D. J. (2010) In vitro screening of environmental chemicals for targeted testing prioritization: the ToxCast project. *Environ. Health Perspect.* 118, 485–492.
- (4) NRC (1984) *Toxicity Testing: Strategies to Determine Needs and Priorities*, National Academies Press, Washington, D.C.
- (5) Keiser, M. J., Setola, V., Irwin, J. J., Laggner, C., Abbas, A. I., Hufeisen, S. J., Jensen, N. H., Kuijter, M. B., Matos, R. C., Tran, T. B., Whaley, R., Glennon, R. A., Hert, J., Thomas, K. L., Edwards, D. D., Shoichet, B. K., and Roth, B. L. (2009) Predicting new molecular targets for known drugs. *Nature* 462, 175–181.
- (6) Xie, L., Xie, L., and Bourne, P. E. (2011) Structure-based systems biology for analyzing off-target binding. *Curr. Opin. Struct. Biol.* 21, 189–199.
- (7) Ankley, G. T., Bennett, R. S., Erickson, R. J., Hoff, D. J., Hornung, M. W., Johnson, R. D., Mount, D. R., Nichols, J. W., Russom, C. L., Schmieder, P. K., Serrano, J. A., Tietge, J. E., and Villeneuve, D. L. (2010) Adverse outcome pathways: a conceptual framework to support ecotoxicology research and risk assessment. *Environ. Toxicol. Chem.* 29, 730–741.
- (8) Martin, M. T., Dix, D. J., Judson, R. S., Kavlock, R. J., Reif, D. M., Richard, A. M., Rotroff, D. M., Romanov, S., Medvedev, A., Poltoratskaya, N., Gambarian, M., Moeser, M., Makarov, S. S., and Houck, K. A. (2010) Impact of environmental chemicals on key transcription regulators and correlation to toxicity end points within EPA's ToxCast program. *Chem. Res. Toxicol.* 23, 578–590.
- (9) Knudsen, T. B., Houck, K. A., Sipes, N. S., Singh, A. V., Judson, R. S., Martin, M. T., Weissman, A., Kleinstreuer, N. C., Mortensen, H. M., Reif, D. M., Rabinowitz, J. R., Setzer, R. W., Richard, A. M., Dix, D. J., and Kavlock, R. J. (2011) Activity profiles of 309 ToxCast chemicals evaluated across 292 biochemical targets. *Toxicology* 282, 1–15.
- (10) Berg, E. L., Kunkel, E. J., Hytopoulos, E., and Plavec, I. (2006) Characterization of compound mechanisms and secondary activities by BioMAP analysis. *J. Pharmacol. Toxicol. Methods* 53, 67–74.
- (11) Giuliano, K. A., Johnston, P. A., Gough, A., and Taylor, D. L. (2006) Systems cell biology based on high-content screening. *Methods Enzymol.* 414, 601–619.
- (12) Rotroff, D. M., Beam, A. L., Dix, D. J., Farmer, A., Freeman, K. M., Houck, K. A., Judson, R. S., LeCluyse, E. L., Martin, M. T., Reif, D. M., and Ferguson, S. S. (2010) Xenobiotic-metabolizing enzyme and transporter gene expression in primary cultures of human hepatocytes modulated by ToxCast chemicals. *J. Toxicol. Environ. Health, Part B* 13, 329–346.
- (13) Chandler, K. J., Barrier, M., Jeffay, S., Nichols, H. P., Kleinstreuer, N. C., Singh, A. V., Reif, D. M., Sipes, N. S., Judson, R. S., Dix, D. J., Kavlock, R., Hunter, E. S., III, and Knudsen, T. B. (2011) Evaluation of 309 environmental chemicals using a mouse embryonic stem cell adherent cell differentiation and cytotoxicity assay. *PLoS One* 6, e18540.
- (14) Huang, R., Xia, M., Cho, M. H., Sakamuru, S., Shinn, P., Houck, K. A., Dix, D. J., Judson, R. S., Witt, K. L., Kavlock, R. J., Tice, R. R., and Austin, C. P. (2011) Chemical genomics profiling of environmental chemical modulation of human nuclear receptors. *Environ. Health Perspect.* 119, 1142–1148.
- (15) Ingles, J., Auld, D. S., Jadhav, A., Johnson, R. L., Simeonov, A., Yasgar, A., Zheng, W., and Austin, C. P. (2006) Quantitative high-throughput screening: a titration-based approach that efficiently identifies biological activities in large chemical libraries. *Proc. Natl. Acad. Sci. U.S.A.* 103, 11473–11478.

- (16) Shukla, S. J., Huang, R., Austin, C. P., and Xia, M. (2010) The future of toxicity testing: a focus on in vitro methods using a quantitative high-throughput screening platform. *Drug Discovery Today* 15, 997–1007.
- (17) Collins, F. S., Gray, G. M., and Bucher, J. R. (2008) Toxicology. Transforming environmental health protection. *Science* 319, 906–907.
- (18) Worth, A. P., Lapenna, S., and Serafimova, R. (2013) QSAR and metabolic assessment tools in the assessment of genotoxicity. *Methods Mol. Biol.* 930, 125–162.
- (19) Judson, R. S., Martin, M. T., Egeghy, P., Gangwal, S., Reif, D. M., Kothiya, P., Wolf, M., Cathey, T., Transue, T., Smith, D., Vail, J., Frame, A., Mosher, S., Cohen Hubal, E. A., and Richard, A. M. (2012) Aggregating data for computational toxicology applications: The U.S. Environmental Protection Agency (EPA) Aggregated Computational Toxicology Resource (ACToR) System. *Int. J. Mol. Sci.* 13, 1805–1831.
- (20) Ihaka, R., and Gentleman, R. (1996) R: A Language for Data Analysis and Graphics. *J. Comp. Graph. Stat.* 5, 299–314.
- (21) R Development Core Team (2012) *R: A Language and Environment for Statistical Computing*, ISBN 3-900051-07-0, R Foundation for Statistical Computing, Vienna, Austria, <http://www.R-project.org>.
- (22) O'Boyle, N. M., Banck, M., James, C. A., Morley, C., Vandermeersch, T., and Hutchison, G. R. (2011) Open Babel: An open chemical toolbox. *J. Cheminform.* 3, 33.
- (23) Yap, C. W. (2011) PaDEL-descriptor: an open source software to calculate molecular descriptors and fingerprints. *J. Comput. Chem.* 32, 1466–1474.
- (24) Cline, M. S., Smoot, M., Cerami, E., Kuchinsky, A., Landys, N., Workman, C., Christmas, R., Avila-Campilo, I., Creech, M., Gross, B., Hanspers, K., Isserlin, R., Kelley, R., Killcoyne, S., Lotia, S., Maere, S., Morris, J., Ono, K., Pavlovic, V., Pico, A. R., Vailaya, A., Wang, P. L., Adler, A., Conklin, B. R., Hood, L., Kuiper, M., Sander, C., Schmulevich, I., Schwikowski, B., Warner, G. J., Ideker, T., and Bader, G. D. (2007) Integration of biological networks and gene expression data using Cytoscape. *Nat. Protoc.* 2, 2366–2382.
- (25) Schmidt, C. J., Fadayel, G. M., Sullivan, C. K., and Taylor, V. L. (1992) 5-HT₂ receptors exert a state-dependent regulation of dopaminergic function: studies with MDL 100,907 and the amphetamine analogue, 3,4-methylenedioxymethamphetamine. *Eur. J. Pharmacol.* 223, 65–74.
- (26) Jiaravuthisan, M. M., Sasseville, D., Vender, R. B., Murphy, F., and Muhn, C. Y. (2007) Psoriasis of the nail: anatomy, pathology, clinical presentation, and a review of the literature on therapy. *J. Am. Acad. Dermatol.* 57, 1–27.
- (27) Jensen, K., Johnson, L. A., Jacobson, P. A., Kachler, S., Kirstein, M. N., Lamba, J., and Klotz, K. N. (2012) Cytotoxic purine nucleoside analogues bind to A1, A2A, and A3 adenosine receptors. *Naunyn-Schmiedeberg's Arch. Pharmacol.* 385, 519–525.
- (28) Witorsch, R. J., and Thomas, J. A. (2010) Personal care products and endocrine disruption: A critical review of the literature. *Crit. Rev. Toxicol.* 40 (Suppl3), 1–30.
- (29) Tickner, J. A., Schettler, T., Guidotti, T., McCally, M., and Rossi, M. (2001) Health risks posed by use of Di-2-ethylhexyl phthalate (DEHP) in PVC medical devices: a critical review. *Am. J. Ind. Med.* 39, 100–111.
- (30) U.S. Consumer Product Safety Commission by Versar, Inc. and Syracuse Research Corporation (SRC) (2010) Review of exposure and toxicity data for phthalate substitutes, www.cpsc.gov/about/cpsia/phthalsub.pdf (accessed Jan 4, 2012).
- (31) Blair, R. M., Fang, H., Branham, W. S., Hass, B. S., Dial, S. L., Moland, C. L., Tong, W., Shi, L., Perkins, R., and Sheehan, D. M. (2000) The estrogen receptor relative binding affinities of 188 natural and xenochemicals: structural diversity of ligands. *Toxicol. Sci.* 54, 138–153.
- (32) Dubois, K. P., Raymund, A. B., and Hietbrink, B. E. (1961) Inhibitory action of dithiocarbamates on enzymes of animal tissues. *Toxicol. Appl. Pharmacol.* 3, 236–255.
- (33) Miller, D. B. (1982) Neurotoxicity of the pesticidal carbamates. *Neurobehav. Toxicol. Teratol.* 4, 779–787.
- (34) O'Carroll, R. E., Masterton, G., Dougall, N., Ebmeier, K. P., and Goodwin, G. M. (1995) The neuropsychiatric sequelae of mercury poisoning. The Mad Hatter's disease revisited. *Br. J. Psychiatry* 167, 95–98.
- (35) Harada, M. (1995) Minamata disease: methylmercury poisoning in Japan caused by environmental pollution. *Crit. Rev. Toxicol.* 25, 1–24.
- (36) Haroon, M., and Fitzgerald, O. (2012) Pathogenetic overview of psoriatic disease. *J. Rheumatol., Suppl.* 89, 7–10.
- (37) Chen, X., Beutler, J. A., McCloud, T. G., Loehfelm, A., Yang, L., Dong, H. F., Chertov, O. Y., Salcedo, R., Oppenheim, J. J., and Howard, O. M. (2003) Tannic acid is an inhibitor of CXCL12 (SDF-1 α)/CXCR4 with antiangiogenic activity. *Clin. Cancer Res.* 9, 3115–3123.
- (38) Di Gennaro, A., and Haeggstrom, J. Z. (2012) The leukotrienes: immune-modulating lipid mediators of disease. *Adv. Immunol.* 116, 51–92.
- (39) Keil, D. E., Mehlmann, T., Butterworth, L., and Peden-Adams, M. M. (2008) Gestational exposure to perfluorooctane sulfonate suppresses immune function in B6C3F1 mice. *Toxicol. Sci.* 103, 77–85.
- (40) Lounkine, E., Keiser, M. J., Whitebread, S., Mikhailov, D., Hamon, J., Jenkins, J. L., Lavan, P., Weber, E., Doak, A. K., Cote, S., Shoichet, B. K., and Urban, L. (2012) Large-scale prediction and testing of drug activity on side-effect targets. *Nature* 486, 361–367.
- (41) Paolini, G. V., Shapland, R. H., van Hoorn, W. P., Mason, J. S., and Hopkins, A. L. (2006) Global mapping of pharmacological space. *Nat. Biotechnol.* 24, 805–815.
- (42) Duax, W. L., Griffin, J. F., Weeks, C. M., and Wawrzak, Z. (1988) The mechanism of action of steroid antagonists: insights from crystallographic studies. *J. Steroid Biochem.* 31, 481–492.
- (43) Tabira, Y., Nakai, M., Asai, D., Yakabe, Y., Tahara, Y., Shinmyozu, T., Noguchi, M., Takatsuki, M., and Shimohigashi, Y. (1999) Structural requirements of para-alkylphenols to bind to estrogen receptor. *Eur. J. Biochem.* 262, 240–245.
- (44) Reigart, J. R., and Roberts, J. R. (1999) N-Methyl Carbamate Insecticides, in *Recognition and Management of Pesticide Poisoning* (Langner, G., Ed.) pp 48–54, U.S. Environmental Protection Agency, Washington, D.C.
- (45) Vilches-Herrera, M., Miranda-Sepulveda, J., Rebolledo-Fuentes, M., Fierro, A., Luhr, S., Iturriaga-Vasquez, P., Cassels, B. K., and Reyes-Parada, M. (2009) Naphthylisopropylamine and N-benzylamphetamine derivatives as monoamine oxidase inhibitors. *Bioorg. Med. Chem.* 17, 2452–2460.
- (46) Sipes, N. S., Martin, M. T., Reif, D. M., Kleinstreuer, N. C., Judson, R. S., Singh, A. V., Chandler, K. J., Dix, D. J., Kavlock, R. J., and Knudsen, T. B. (2011) Predictive models of prenatal developmental toxicity from ToxCast high-throughput screening data. *Toxicol. Sci.* 124, 109–127.
- (47) Martin, M. T., Knudsen, T. B., Reif, D. M., Houck, K. A., Judson, R. S., Kavlock, R. J., and Dix, D. J. (2011) Predictive model of rat reproductive toxicity from ToxCast high throughput screening. *Biol. Reprod.* 85, 327–339.
- (48) Oishi, K., Toyao, K., and Kawano, Y. (2008) Suppression of estrogenic activity of 17-beta-estradiol by beta-cyclodextrin. *Chemosphere* 73, 1788–1792.
- (49) Del Valle, E. M. M. (2004) Cyclodextrins and their uses: a review. *Process Biochem. (Oxford, U. K.)* 39, 1033–1046.
- (50) Wetmore, B. A., Wambaugh, J. F., Ferguson, S. S., Sochaski, M. A., Rotroff, D. M., Freeman, K., Clewell, H. J., III, Dix, D. J., Andersen, M. E., Houck, K. A., Allen, B., Judson, R. S., Singh, R., Kavlock, R. J., Richard, A. M., and Thomas, R. S. (2012) Integration of dosimetry, exposure, and high-throughput screening data in chemical toxicity assessment. *Toxicol. Sci.* 125, 157–174.
- (51) Dix, D. J., Houck, K. A., Judson, R. S., Kleinstreuer, N. C., Knudsen, T. B., Martin, M. T., Reif, D. M., Richard, A. M., Shah, I., Sipes, N. S., and Kavlock, R. J. (2012) Incorporating biological,

chemical, and toxicological knowledge into predictive models of toxicity. *Toxicol. Sci.* 130, 440–441. author reply 442–443.

(52) Knudsen, T. B., and Kleinstreuer, N. C. (2011) Disruption of embryonic vascular development in predictive toxicology. *Birth Defects Res., Part C* 93, 312–323.

(53) Kleinstreuer, N., Dix, D., Rountree, M., Baker, N., Sipes, N., Reif, D., Spencer, R., and Knudsen, T. (2013) A computational model predicting disruption of blood vessel development. *PLoS Comput. Biol.* 9, e1002996.

(54) Kleinstreuer, N. C., and Knudsen, T. B. (2011) Predictive Modeling and Computational Toxicology, in *Developmental and Reproductive Toxicology: A Practical Approach* (Hood, R. D., Ed.) pp 578–591, Informa Healthcare Books, London, U.K.

(55) Hals, P. A., Hall, H., and Dahl, S. G. (1988) Muscarinic cholinergic and histamine H1 receptor binding of phenothiazine drug metabolites. *Life Sci.* 43, 405–412.

(56) Huerta-Bahena, J., Villalobos-Molina, R., and Garcia-Sainz, J. A. (1983) Trifluoperazine and chlorpromazine antagonize alpha 1- but not alpha2- adrenergic effects. *Mol. Pharmacol.* 23, 67–70.

(57) Trichard, C., Paillere-Martinot, M. L., Attar-Levy, D., Recassens, C., Monnet, F., and Martinot, J. L. (1998) Binding of antipsychotic drugs to cortical 5-HT2A receptors: a PET study of chlorpromazine, clozapine, and amisulpride in schizophrenic patients. *Am. J. Psychiatry* 155, 505–508.

(58) York, D. H. (1972) Dopamine receptor blockade—a central action of chlorpromazine on striatal neurones. *Brain Res.* 37, 91–99.

(59) Arnt, J., and Skarsfeldt, T. (1998) Do novel antipsychotics have similar pharmacological characteristics? A review of the evidence. *Neuropsychopharmacology* 18, 63–101.

(60) Tam, S. W., and Cook, L. (1984) Sigma opiates and certain antipsychotic drugs mutually inhibit (+)-[3H] SKF 10,047 and [3H]haloperidol binding in guinea pig brain membranes. *Proc. Natl. Acad. Sci. U.S.A.* 81, 5618–5621.

(61) Tuppurainen, H., Kuikka, J. T., Viinamaki, H., Husso, M., and Tiihonen, J. (2009) Dopamine D2/3 receptor binding potential and occupancy in midbrain and temporal cortex by haloperidol, olanzapine and clozapine. *Psychiatry Clin. Neurosci.* 63, 529–537.

(62) McCort, G., Hoornaert, C., Aletru, M., Denys, C., Duclos, O., Cadilhac, C., Guilpain, E., Dellac, G., Janiak, P., Galzin, A. M., Delahaye, M., Guilbert, F., and O'Connor, S. (2001) Synthesis and SAR of 3- and 4-substituted quinolin-2-ones: discovery of mixed 5-HT(1B)/5-HT(2A) receptor antagonists. *Bioorg. Med. Chem.* 9, 2129–2137.

(63) LaFrata, A. L., Carlson, K. E., and Katzenellenbogen, J. A. (2009) Steroidal bivalent ligands for the estrogen receptor: design, synthesis, characterization and binding affinities. *Bioorg. Med. Chem.* 17, 3528–3535.

(64) Yeh, S., Miyamoto, H., Shima, H., and Chang, C. (1998) From estrogen to androgen receptor: a new pathway for sex hormones in prostate. *Proc. Natl. Acad. Sci. U.S.A.* 95, 5527–5532.

(65) Rider, C. V., Hartig, P. C., Cardon, M. C., and Wilson, V. S. (2009) Comparison of chemical binding to recombinant fathead minnow and human estrogen receptors alpha in whole cell and cell-free binding assays. *Environ. Toxicol. Chem.* 28, 2175–2181.

(66) Planting, A., van der Gaast, A., Schoffski, P., Bartkowski, M., Verheij, C., Noe, D., Ferrante, K., and Verweij, J. (2005) A phase I and pharmacologic study of the matrix metalloproteinase inhibitor CP-471,358 in patients with advanced solid tumors. *Cancer Chemother. Pharmacol.* 55, 136–142.

(67) Dalvie, D., Cosker, T., Boyden, T., Zhou, S., Schroeder, C., and Potchoiba, M. J. (2008) Metabolism distribution and excretion of a matrix metalloproteinase-13 inhibitor, 4-[4-(4-fluorophenoxy)-benzenesulfonylamino]tetrahydropyran-4-carboxylic acid hydroxamide (CP-544439), in rats and dogs: assessment of the metabolic profile of CP-544439 in plasma and urine of humans. *Drug Metab. Dispos.* 36, 1869–1883.

(68) Shiau, A. K., Barstad, D., Loria, P. M., Cheng, L., Kushner, P. J., Agard, D. A., and Greene, G. L. (1998) The structural basis of estrogen

receptor/coactivator recognition and the antagonism of this interaction by tamoxifen. *Cell* 95, 927–937.

(69) Gaido, K. W., Leonard, L. S., Maness, S. C., Hall, J. M., McDonnell, D. P., Saville, B., and Safe, S. (1999) Differential interaction of the methoxychlor metabolite 2,2-bis-(p-hydroxyphenyl)-1,1,1-trichloroethane with estrogen receptors alpha and beta. *Endocrinology* 140, 5746–5753.

(70) Watson, N., Reddy, H., Stefanich, E., and Eglen, R. M. (1995) Characterization of the interaction of zamifenacin at muscarinic receptors in vitro. *Eur. J. Pharmacol.* 285, 135–142.

(71) Watson, N., Daniels, D. V., Ford, A. P., Eglen, R. M., and Hegde, S. S. (1999) Comparative pharmacology of recombinant human M3 and M5 muscarinic receptors expressed in CHO-K1 cells. *Br. J. Pharmacol.* 127, 590–596.

(72) Pasternak, G. W., Snowman, A. M., and Snyder, S. H. (1975) Selective enhancement of [3H]opiate agonist binding by divalent cations. *Mol. Pharmacol.* 11, 735–744.

(73) Williams, S. P., and Sigler, P. B. (1998) Atomic structure of progesterone complexed with its receptor. *Nature* 393, 392–396.

(74) Emonds-Alt, X., Advenier, C., Cognon, C., Croci, T., Daoui, S., Ducoux, J. P., Landi, M., Naline, E., Neliat, G., Poncelet, M., Proietto, V., Van Broeck, D., Vilain, P., Soubrie, P., Le Fur, G., Maffrand, J. P., and Breliere, J. C. (1997) Biochemical and pharmacological activities of SR 144190, a new potent non-peptide tachykinin NK2 receptor antagonist. *Neuropeptides* 31, 449–458.

(75) Ishizaki, H., Yamada, S., Yanagiguchi, K., Koyama, Z., Ikeda, T., and Hayashi, Y. (2009) Pre-treatment with tannic acid inhibits the intracellular IL-8 production by chitosan in a human oral epithelial cancer cell line. *Oral Med. Pathol.* 13, 135–141.

(76) Amitai, G., Moorad, D., Adani, R., and Doctor, B. P. (1998) Inhibition of acetylcholinesterase and butyrylcholinesterase by chlorpyrifos-oxon. *Biochem. Pharmacol.* 56, 293–299.

(77) Showell, H. J., Pettipher, E. R., Cheng, J. B., Breslow, R., Conklyn, M. J., Farrell, C. A., Hingorani, G. P., Salter, E. D., Hackman, B. C., Wimberly, D. J., et al. (1995) The in vitro and in vivo pharmacologic activity of the potent and selective leukotriene B4 receptor antagonist CP-105696. *J. Pharmacol. Exp. Ther.* 273, 176–184.

(78) Butler, S., Hall, F. R., and Sanford, H. N. (1950) An investigation of the mode of action of benadryl as an antihistaminic. *J. Lab. Clin. Med.* 36, 806.

(79) Rago, B., Liu, J., Tan, B., and Holliman, C. (2011) Application of the dried spot sampling technique for rat cerebrospinal fluid sample collection and analysis. *J. Pharm. Biomed. Anal.* 55, 1201–1207.

(80) Bednar, M., Chieffo, C., Morse, T., Duplin, M., and Gibbs, M. (2004) Plasma and cerebrospinal fluid (CSF) pharmacokinetics of CP-457,920, a selective alpha 5 GABA-A receptor inverse agonist in young, healthy volunteers. *Clin. Pharmacol. Ther.* 75, 90.

(81) Gauthier, D. R., Jr., Limanto, J., Devine, P. N., Desmond, R. A., Szumigala, R. H., Jr., Foster, B. S., and Volante, R. P. (2005) Palladium-catalyzed regioselective arylation of imidazo[1,2-b][1,2,4]-triazine: synthesis of an alpha 2/3-selective GABA agonist. *J. Org. Chem.* 70, 5938–5945.

(82) Zhu, C., Hansen, A. R., Bateman, T., Chen, Z., Holt, T. G., Hubert, J. A., Karanam, B. V., Lee, S. J., Pan, J., Qian, S., Reddy, V. B., Reitman, M. L., Strack, A. M., Tong, V., Weingarth, D. T., Wolff, M. S., MacNeil, D. J., Weber, A. E., Duffy, J. L., and Edmondson, S. D. (2008) Discovery of imidazole carboxamides as potent and selective CCK1R agonists. *Bioorg. Med. Chem. Lett.* 18, 4393–4396.

(83) McLean, S., Ganong, A., Seymour, P. A., Bryce, D. K., Crawford, R. T., Morrone, J., Reynolds, L. S., Schmidt, A. W., Zorn, S., Watson, J., Fossa, A., DePasquale, M., Rosen, T., Nagahisa, A., Tsuchiya, M., and Heym, J. (1996) Characterization of CP-122,721; a nonpeptide antagonist of the neurokinin NK1 receptor. *J. Pharmacol. Exp. Ther.* 277, 900–908.

(84) Kelly, J. (2009) Appendices, in *Principles of CNS Drug Development: From Test Tube to Patient* pp 287–293, John Wiley & Sons, Ltd., Chichester, U.K.

(85) Metro, T. X., Cochi, A., Gomez Pardo, D., and Cossy, J. (2011) Asymmetric synthesis of an antagonist of neurokinin receptors: SSR 241586. *J. Org. Chem.* 76, 2594–2602.

(86) Croci, T., Cecchi, R., Marini, P., Rouget, C., Viviani, N., Germain, G., Guagnini, F., Fradin, Y., Descamps, L., Pascal, M., Advenier, C., Breuiller-Fouche, M., Leroy, M. J., and Bardou, M. (2007) In vitro and in vivo pharmacological characterization of ethyl-4-[trans-4-[(2S)-2-hydroxy-3-[4-hydroxy-3[(methylsulfonyl)amino]phenoxy]propyl]amino]cyclohexyl]benzoate hydrochloride (SAR150640), a new potent and selective human beta3-adrenoceptor agonist for the treatment of preterm labor. *J. Pharmacol. Exp. Ther.* 321, 1118–1126.

(87) Walsh, S. L., Strain, E. C., Abreu, M. E., and Bigelow, G. E. (2001) Enadoline, a selective kappa opioid agonist: comparison with butorphanol and hydromorphone in humans. *Psychopharmacology (Berlin, Ger.)* 157, 151–162.

(88) Gray, J. A., and Roth, B. L. (2007) The pipeline and future of drug development in schizophrenia. *Mol. Psychiatry* 12, 904–922.

(89) Mente, S., Gallaschun, R., Schmidt, A., Lebel, L., Vanase-Frawley, M., and Fliri, A. (2008) Quantitative structure-activity relationship of phenoxyphenyl-methanamine compounds with 5HT_{2A}, SERT, and hERG activities. *Bioorg. Med. Chem. Lett.* 18, 6088–6092.

(90) Middleton, D. S., Andrews, M., Glossop, P., Gymer, G., Hepworth, D., Jessiman, A., Johnson, P. S., MacKenny, M., Stobie, A., Tang, K., Morgan, P., and Jones, B. (2008) Designing rapid onset selective serotonin re-uptake inhibitors. Part 3: Site-directed metabolism as a strategy to avoid active circulating metabolites: structure-activity relationships of (thioalkyl)phenoxy benzylamines. *Bioorg. Med. Chem. Lett.* 18, 5303–5306.

(91) Bromidge, S. M., Dabbs, S., Davies, D. T., Davies, S., Duckworth, D. M., Forbes, I. T., Gaster, L. M., Ham, P., Jones, G. E., King, F. D., Mulholland, K. R., Saunders, D. V., Wyman, P. A., Blaney, F. E., Clarke, S. E., Blackburn, T. P., Holland, V., Kennett, G. A., Lightowler, S., Middlemiss, D. N., Trail, B., Riley, G. J., and Wood, M. D. (2000) Biarylcarbamoylindolines are novel and selective 5-HT_{2C} receptor inverse agonists: identification of 5-methyl-1-[[2-[(2-methyl-3-pyridyl)oxy]-5-pyridyl]carbamoyl]-6-trifluoromethylindoline (SB-243213) as a potential antidepressant/anxiolytic agent. *J. Med. Chem.* 43, 1123–1134.

(92) Knight, A. R., Misra, A., Quirk, K., Benwell, K., Revell, D., Kennett, G., and Bickerdike, M. (2004) Pharmacological characterisation of the agonist radioligand binding site of 5-HT_{2A}, 5-HT_{2B} and 5-HT_{2C} receptors. *Naunyn-Schmiedeberg's Arch. Pharmacol.* 370, 114–123.

(93) Ashcroft, F. J., Newberg, J. Y., Jones, E. D., Mikic, I., and Mancini, M. A. (2011) High content imaging-based assay to classify estrogen receptor-alpha ligands based on defined mechanistic outcomes. *Gene* 477, 42–52.

(94) Luo, G., Cunningham, M., Kim, S., Burn, T., Lin, J., Sinz, M., Hamilton, G., Rizzo, C., Jolley, S., Gilbert, D., Downey, A., Mudra, D., Graham, R., Carroll, K., Xie, J., Madan, A., Parkinson, A., Christ, D., Selling, B., LeCluyse, E., and Gan, L. S. (2002) CYP3A4 induction by drugs: correlation between a pregnane X receptor reporter gene assay and CYP3A4 expression in human hepatocytes. *Drug Metab. Dispos.* 30, 795–804.

(95) Le Fur, G., Vaucher, N., Perrier, M. L., Flamier, A., Benavides, J., Renault, C., Dubroeuq, M. C., Guerey, C., and Uzan, A. (1983) Differentiation between two ligands for peripheral benzodiazepine binding sites, [3H]RO5-4864 and [3H]PK 11195, by thermodynamic studies. *Life Sci.* 33, 449–457.